FILE

INTERNAL DOCUMENT 219

I.O.S.

CONFIDENTIAL

PREDICTABILITY OF SURFACE WAVE SPECTRA FROM A PARAMETRIC SPECTRAL MODEL

by

SASITHORN ARANUVACHUPUN

Internal Document No 219

[*This document should not be cited in a published bibliography, and is supplied for the use of the recipient only*].

NATURAL ENVIRONMENT RESEARCH COUNCIL

INSTITUTE OF OCEANOGRAPHIC SCIENCES

INSTITUTE OF OCEANOGRAPHIC SCIENCES

Wormley, Godalming,
Surrey GU8 5UB
(042-879-4141)

(Director: Dr. A. S. Laughton)

Bidston Observatory,
Birkenhead,
Merseyside L43 7RA
(051-653-8633)
(Assistant Director: Dr. D. E. Cartwright)

Crossway,
Taunton,
Somerset TA1 2DW
(0823-86211)
(Assistant Director: M. J. Tucker)

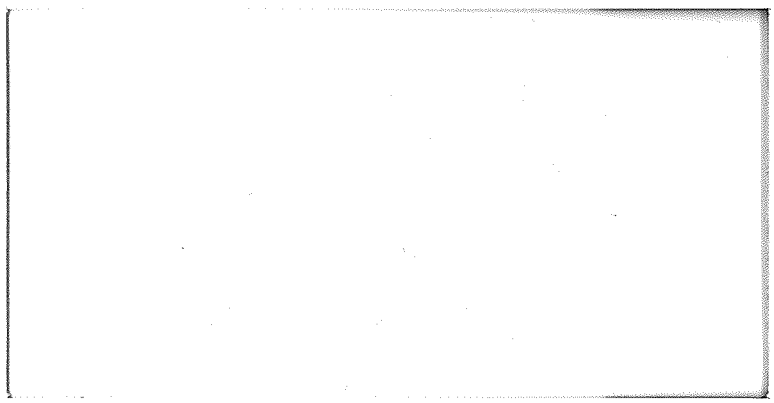

PREDICTABILITY OF SURFACE WAVE SPECTRA FROM A PARAMETRIC SPECTRAL MODEL

by

SASITHORN ARANUVACHUPUN

Internal Document No 219

This document should not be cited in any other paper or report except as 'personal communication' and it is for the use of the recipient only

Institute of Oceanographic Sciences
Crossway
Taunton
Somerset TA1 2DW

September 1984

CONTENTS

1. INTRODUCTION

Since the application of spectral concepts were introduced to describe ocean waves, a great deal of effort has been put into spectral modelling of the waves. Such efforts have considerable benefits in the design of ships, offshore structures and coastal engineering. Evaluating the predictability of measured wave spectra also provides improvements to the methods of practical prediction from meteorological data.

The two most widely used models are that developed by Pierson and Moskowitz (1964 for a "fully-arisen sea" and that developed by Hasselmann et al (1976) as a result of the Joint North Sea Wave Project. This "JONSWAP" model includes short fetches and durations and is therefore more general. It is therefore used in this study.

The study is divided into two parts. In the first part, simulation of highly variable wave spectra (including the natural randomness) from a given mean JONSWAP spectrum was carried out. Then the JONSWAP formula was fitted to the simulated spectra to recover the spectral parameters in order to examine the fitting procedure. It is found that the usual method produces a major bias in the γ parameter if applied to 1000 s wave records. The bias reduces only slowly as the record length is increased.

In the second part of the study, a storm is examined using continuous digital recordings from a Waverider moored in 100 m of water west of the Scilly Isles. The objective of this is to see whether the spectrum at the peak of a severe storm approximates to either the JONSWAP or Pierson-Moskowitz formulae.

2. SIMULATED WAVE SPECTRA

(i) Simulation of spectral densities

The simulation is based on the Monte Carlo method. A discrete power spectrum is considered, ie at each discrete harmonic frequency f_k, there is a corresponding spectral density C_k, $k = 1, 2, \ldots\ldots \ell$. The spectral density $\hat{C}_k$ calculated from a finite measured record is known as the spectral estimator and is defined as

$$\hat{C}\ (f_i)\quad \delta f = \frac{1}{2}\ \{A^2(f_i) + B^2(f_i)\}$$

where δf is the frequency interval between harmonics ie δf = 1/record length = $1/N\Delta$ The Gaussian process h_t, has N numbers of data points in the record with Δ time interval between them. The Fourier components $A(f_i)$ and $B(f_i)$ of the ith harmonic are written as

$$A(f_i) = \frac{2}{N} \sum_{n=1}^{N} h_n \cos 2\pi f_i n \qquad B(f_i) = \frac{2}{N} \sum_{n=1}^{N} h_n \sin 2\pi f_i n$$

where $f_i = i\ \delta f$

The components $A(f_i)$ and $B(f_i)$ are normally distributed random variables with a variance of $S(f)\,\delta f$ where $S(f)$ is the true spectral density. To obtain ν degrees of freedom, the spectral estimator is averaged over $\nu/2$ adjacent harmonics. Thus, the above expression now becomes

$$\hat{C}\,(f_k) = \frac{N\Delta}{\nu} \sum_{i\,=\,k\,-\nu/2}^{(k\,+\,\nu/2)\,-1} \{A^2(f_i) + B^2(f_i)\} \quad .$$

Notice that the summation is essentially the variance $S(f_k)$ and is a chi-squared distribution with ν degrees of freedom. Therefore, the spectral estimator can be written as

$$\hat{C}(f_k) = \frac{S(f_k)}{\nu} \quad .$$

If a random variable (rv) is defined as (Jenkins & Watts 1968)

$$Z(f_k) = \frac{\nu C(f_k)}{S(f_k)} \quad , \tag{1}$$

the rv also has a chi-squared distribution with ν degrees of freedom and the spectral estimator of the form

$$\hat{C}(f_k) = \frac{S(f_k)\; Z(f_k)}{\nu} \quad . \tag{2}$$

We now let the true spectrum $S(f_k)$ be the mean JONSWAP spectrum with the following parameter values: $\alpha = 0.0162$, $f_m = 0.364$, $\gamma = 3.3$, $\sigma_a = 0.07$ and $\sigma_b = 0.09$. The rv $Z(f_k)$ is simulated on the NERC computer system (Honeywell 66/DPS-300 using the NAG random number generator. A pseudo-random real number is taken from a chi squared distribution with ν degrees of freedom. Then, the sample spectral density is estimated using equation (2). The simulation is carried out for 50 frequencies ranging from 0.1427 to 0.4900 Hz at the frequency resolution of 0.0098 Hz, and for 20, 40 and 80 degrees of freedom. The parameter values and conditions for the simulation are selected such that a direct comparison between the simulated and measured spectra can be pursued. Examples of the simulated spectra may be seen in Figs 1-3. The simulated spectral density is plotted against the frequency by the dashed line while the solid line represents the mean JONSWAP spectrum which has been assumed to be the population (theoretical) spectrum of the simulation. Figures 1-3 are for 20, 40 and 80 degrees of freedom respectively with the same initial state for the pseudo-random real number generator which generates the rv $Z(f_k)$.

(ii) Application of parametric spectral models

Each of the simulated spectrum is fitted by the JONSWAP spectral model of the form

$$E_J(f) = \alpha g^2 (2\pi)^{-4} f^{-5} \exp\{-\frac{5}{4}(\frac{f}{f_m})^{-4} + \ln\gamma \exp\{-\frac{(f-f_m)^2}{2\sigma^2 f_m^2}\}\} \quad (3)$$

where

$\sigma = \sigma_a$ if $f < f_m$

$\sigma = \sigma_b$ if $f \geq f_m$

Notice that the JONSWAP spectral model contains two scale parameters namely,

α = Phillip's constant

f_m = peak frequency

and three shape parameters namely,

γ = peak enhancement factor

σ_a = left peak width

σ_b = right peak width

For $\gamma = 1$, the JONSWAP spectrum reduces to the Pierson-Moskowitz spectrum for fully developed sea which can be expressed as (Pierson & Moskowitz 1964)

$$E_{PM}(f) = \alpha g^2 (2\pi)^{-4} f^{-5} \exp\{-\frac{5}{4}(\frac{f}{f_m})^{-4}\} \quad (4)$$

The details of JONSWAP parameter determination may be found in Günther (1981). Briefly, the peak region of a measured spectrum is fitted by a parabolic function whose derivative with respect to frequency is computed. Where the derivative approaches zero, the frequency is taken as f_m and the peak value is used to estimate γ. The Pierson-Moskowitz spectrum (equation (4)) is fitted to the measured spectrum in the frequency range $1.35 f_m < f < 2f_m$, to estimate α. Then the ratio between the peak value and the corresponding Pierson-Moskowitz peak value provides the value of γ. The same method is applied to determine the values of α, f_m and γ for each simulated spectrum. The parameters σ_a and σ_b are however, determined by a least square method using the following expression for minimization

$$F(f) = \sum_{f=f_1}^{f_2} \{E_J(f) - E_S(f)\}^2 \quad , \quad f_1 \geq 0,\ f_2 > f_m; \quad \text{for } \sigma_a$$

$$\text{and } f_1 \geq f_m,\ f_2 < f_{N/2}: \quad \text{for } \sigma_b \quad ,$$

where $E_S(f)$ is the simulated spectral density at each discrete frequency, which is essentially the same quantity as $C(f_k)$ in equation (2). All the five parameters are determined from the simulated spectrum. The JONSWAP spectrum given by these parameters in the form of equation (3) is plotted by the dotted line in Figs 1-3. A comparison between the simulated (dashed line) and the fitted JONSWAP spectrum (dotted line) shows how well the spectral model (equation (3)) describes a power spectrum of a random process. Notice the the JONSWAP spectrum is a smooth function and therefore it cannot provide more than one peak in the spectrum. This is why only the highest peak of the highly variable spectra simulated, is fitted by the JONSWAP spectral peak. The secondary peak of the simulated spectra is generally ignored. However, the peak frequency f_m is generally in a good agreement with the simulated one indicating that the determination of f_m is an accurate estimate. Also, it should be pointed out that as the degrees of freedom ν in the simulation increase, the simulated spectra become smoother (see Figs 1-3) and hence, the JONSWAP spectral fitting yields better results.

Since the JONSWAP spectrum is basically derived from the Pierson-Moskowitz spectrum (see equation (4)) for fully developed sea, multiplied with the peak-enhancement function

$$\gamma \exp\{-\frac{(f - f_m)^2}{2\sigma^2 f_m^2}\} \quad ,$$

the Pierson-Moskowitz spectrum should also be examined in comparison with the JONSWAP spectrum. Figure 4 shows the same simulation as in Fig 3 (80 degrees of freedom) except the simulated spectrum is fitted by the Pierson-Moskowitz spectrum (in dotted line). It can be seen that the fitted spectral peak has been reduced substantially. This significant difference between the JONSWAP and Pierson-Moskowitz spectrum deserves an explanation which will be discussed in the following section.

(iii) Results and discussion

The original form of the Pierson-Moskowitz spectrum is

$$S(\omega) = \alpha g^2 (2\pi)^{-4} \omega^{-5} \exp\{-\beta(\omega_o/\omega)^4\} \quad , \qquad (5)$$

where $\alpha = 0.0081$, $\beta = 0.74$ and $\omega_o = g/2\pi u$ (Pierson & Moskowitz 1964; Pierson 1977). Notice that the quantity ω_o is the wind speed (u) related frequency and it is not the

same as the peak frequency f_m in the JONSWAP spectrum while frequency ω is exactly the same as frequency f in JONSWAP. In fact, ω_o can be interpreted as the wave response frequency to wind input in the fully developed sea. However, changing the variable ω_o to f_m requires that

$$\frac{d}{d\omega} S(\omega) = o = \frac{S(\omega)}{\omega} \{4\beta(\frac{\omega_o}{\omega})^4 - 5\} ,$$

which is the definition of peak frequency f_m. Thus, for the above condition where ω becomes f_m, the relationship between ω_o and f_m is

$$\omega_o^4 = \frac{5}{4} \beta^{-1} f_m^4 \quad . \tag{6}$$

By substituting ω_o (equation (6)) and $\omega = f$ into equation (5), the spectrum E_{PM} (equation (4)) can be obtained. It is worth pointing out in this analysis that the relationship (6) implies $f_m < \omega_o$ or $f_m/\omega_o < 1$. If this relationship is geophysically real and meaningful, a direct comparison of the parameters α and f_m between JONSWAP and Pierson-Moskowizt spectrum is necessary. A study of Pierson (1977) suggests that the comparison of α from both spectra (α_J/α_{PM}) can be written as

$$\frac{\alpha_J}{\alpha_{PM}} = \exp\{0.1588 (1 - K_m^{-4})\} \{1 + 0.0080 (1 - K_m^{-4}) + 0.00278 (1 - K_m^{-4})^2\}$$

where $K_m = f_m/f_{PM}$ and f_{PM} is given by (see Pierson 1977)

$$f_{PM} = (2\pi)^{-1} (4\beta/5)^{\frac{1}{4}} gu^{-1}$$

It has been pointed out that $\alpha_J = \alpha_{PM}$ only if $K_m = 1$ and $\alpha_J > \alpha_{PM}$ if $K_m > 1$. Notice however that $\alpha_J < \alpha_{PM}$ if $K_m < 1$. Since the parameter γ is defined as a ratio of the peak value of a spectrum to the peak value of the corresponding Pierson-Moskowitz spectrum, the parameter can be overestimated if the Pierson-Moskowitz peak value is underestimated. This situation can happen because of the small value of α. In other words, if $f_m < f_{PM}$ $(K_m < 1)$ similar to $f_m < \omega_o$, and α used in JONSWAP is underestimated $(\alpha_J < \alpha_{PM})$, then the parameter γ will be overestimated. Thus, it can be argued that γ is always greater than unity and the JONSWAP spectrum will never reduce to Pierson-Moskowitz spectrum for real wave fields. The argument is supported by the study of Pierson (1977) where the data of Moskowitz (1964) which has been used to fit the Pierson-Moskowitz spectrum, was reanalysed and refitted to the JONSWAP

spectrum. It is found that the resulting value of γ is 1.40 (Pierson 1977). Furthermore, Liu (1983) has found from his wave data that the parameter γ does not necessarily approach unity as waves approach a fully developed stage.

When the definitions of both parameters f_m and f_{PM} (or ω_o) are recalled, it is clear that the two parameters are not the same. The parameter f_m is derived from a measured wave spectrum where the derivative of the spectrum with respect to frequency is zero while the parameter f_{PM} is the wind related frequency. However, if the relationship between the two parameters (equation (6)) is geophysically real, then the JONSWAP spectrum should be able to reduce to Pierson-Moskowitz spectrum under the fully developed stage. Since this case does not occur as suggested by Pierson (1977) and Liu (1983), it implies that such a relationship is inaccurate and geophysically meaningless for the actual wave environment. Thus, both JONSWAP and Pierson-Moskowitz spectra should be treated as independent spectra. Also notice that the Pierson-Moskowitz spectrum is highly sensitive to the wind speed via f_{PM} (or ω_o) and a slight change in wind speed can cause a significant variation in the spectrum (Pierson 1964).

A fitting of the JONSWAP spectrum has been made to each sixty simulated wave spectra with 20, 40 and 80 degrees of freedom. Although in double peak situation, the fitting does not always yield satisfactory results, better results are generally obtained in the single peak spectra. The resulting JONSWAP parameter values were used to compute basic statistical properties such as mean, variance and correlation coefficient. Table 1 contains means and variances of the five parameters calculated from 60 sample size. It can be seen that among the five parameters, γ has the largest variance while α has the smallest variance. These two parameters are also most sensitive to the change in degrees of freedom. As the degrees of freedom increase from 20 to 40 and 80, the variances of α and γ decrease respectively by 35.09%, 76.29%; and 55.20%, 76.19% of their corresponding variances at 20 degrees of freedom. This decrease of variance is also found in other parameters. Thus, the result indicates that as the spectra get smoother with higher degrees of freedom, the random variability of the parameters is reduced. Furthermore, the parameter γ is not only highly variable due to the large variance but it is also sensitive to the statistical variability. Although the similar sensitivity is found in α, the small variance tends to keep the parameter less variable than γ. Table 1 also suggests that the value of γ has a positive bias although the increase of the degrees of freedom slowly reduces the bias.

The correlation coefficients between various parameters are tabulated in Tables 2, 3 and 4 for 20, 40 and 80 degrees of freedom respectively. In Table 2, the correlation coefficient between f_m and σ_a is the only significant coefficient which has the value as high as 0.84. This is consistent with the results of

Gunther (1981). Figure 5 shows the parameter f_m plotted against the parameter σ_a at zero means (the means of both parameters have been removed). Notice the step-like character of the plot which may be due to the double-peaked spectra where only the highest peak is used to determine f_m. The method is accurate when the highest peak is also the dominant peak of the spectrum. However, when the highest peak is not the dominant peak, a small error can be introduced in f_m and therefore, it could cause a small jump in the values of f_m. Nevertheless, the significant correlation coefficient shown in Fig 5 implies that for low peak frequency waves, the forward face of the spectrum has steeper slope than the high peak frequency waves. Thus, for a wave spectrum which has a low peak frequency f_m, the spectrum tends to be narrower than the spectrum with a high peak frequency. As the degrees of freedom increase and the simulated spectra get smoother, more significant correlation coefficients can be found. For instance, the coefficients for f_m and σ_b, γ and σ_b are also found to be significant in Table 3. Notice that the negative coefficient for f_m and σ_b indicates that as the peak frequency moves toward the high frequency end and the value of σ_a has increased, the value of σ_b will decrease but with a slightly slower rate than the increase of σ_a since the coefficient -0.83 is slightly lower than 0.89. Figures 6 and 7 show similar plots to Fig 5 except for 40 and 80 degrees of freedom respectively. Figures 8 and 9 show the values of γ plotted against the values of σ_b for 40 and 80 degrees of freedom. Once again, the negative coefficient for γ and σ_b indicates that the steeper the spectral tail (or the backward face of the spectrum) becomes,due to the small σ_b, the greater the departure between the JONSWAP and Pierson-Moskowitz spectral peaks. Notice further that additional coefficients are found for H_s and T_z, H_s and spectral band width SBW, T_z and SBW, in Table 4. The coefficients suggest that as waves get bigger with larger period, the spectral band width of the waves becomes smaller, which is consistent with the coefficient of f_m and σ_a.

3. MEASURED WAVE SPECTRA

(iv) Scilly Isles continuous wave data

The wave data was collected from a Waverider buoy deployed at 49° 51' 48" N, 06° 41' 00" W in water depth of 100 m. Although the site was commissioned in October 1979, reliable data was not obtained until February 1980. In this study however, there are only two sets of the wave data during the storms of December 1981, which have been examined in detail. Figure 10 shows the time series of H_s and power of the waves recorded during the months of November and December 1981. The first set of data is from 18-21 December (record numbers 129-470) and the second set is from 25-28 December (record number 762-1056). The measurements for the data were continuous with a sampling interval of half a second. The data format is digital with a record length of 2048 data points. After the instrument calibration, each wave data record was Fourier transformed into a wave power spectrum

which has 20 degrees of freedom. Since it has been shown in the spectral simulation study that the smoother the spectrum, the better the results of JONSWAP spectral fit; the computed wave spectra from the measurements at Scilly Isles have been averaged over four spectra to provide smooth spectra of 80 degrees of freedom. Notice that each of these smooth spectra corresponds to a data record of 68 minutes long and so it will also be termed as the hourly spectrum. Figures 11 and 12 illustrat examples of the hourly spectra obtained from both sets of wave data.

Corresponding wind data was also acquired from a meteorological station at the RAF Mountbatten in Plymouth. For the first set of wave data, the hourly mean of wind speed got up to approximately 12 m s^{-1} in the north-northeast direction. As the wind direction turned from north to south, the hourly mean speed dropped to nearly 3 m s^{-1}, then increased to the maximum of 16 m s^{-1}. The maximum speed of gust was 30 m s^{-1} in the southerly direction. A time series of wind speed during this first storm may be seen in Fig 13 while Fig 14 shows a similar time series but for the second storm corresponding to the second set of wave data. It is interesting to note that during the second storm, the maximum hourly mean of wind speeds got up to 12 m s^{-1} with the maximum speed of gust at 20 m s^{-1} in the southly direction. Since both storms provide strong winds in the dominant north and south directions, it is not unreasonable to compare the wave data from Scilly Isles to the wind data from Plymouth.

(v) Application of JONSWAP model

A fitting of the JONSWAP spectrum to an hourly spectrum measured at Scilly Isles was carried out. All the five JONSWAP parameters were estimated as described in section (ii) 'Application of parametric spectral models'. Figures 15 and 16 show a comparison between the measured hourly spectra (in solid time) and the corresponding fitted JONSWAP spectra (in dashed line) for the first and second storms respectively. The time series of the hourly spectra typically represent the active wind generated waves under the strong wind condition (see also Fig 12 for example). As the wind waves grow under the strong wind forcing, the dominant spectral peak tends to shift toward higher frequency and therefore, double-peaked spectra are often found during active wave generation as well as a fully developed sea. The spectral peak however, returns to lower frequency after the generation has decayed, and the single-peaked spectra appear again. It is the double-peaked spectra which make the fitting of JONSWAP spectrum yield unsatisfactory results as may be seen in Fig 16. Nevertheless, if only the single-peaked spectra are considered, the JONSWAP parameters provide interesting results which will be discussed in the following section.

(vi) JONSWAP parameters

Assuming that the number of double-peaked spectra is small so that the JONSWAP spectral fit generally yields satisfactory results as may be seen in Fig 15; The time series of the value of α obtained from the hourly spectra for the first storm, is presented in Fig 19. For comparison, the corresponding time series of wind speed illustrating the variability of wind forcing during the storm is also presented in the same figure. It can be seen that there is a remarkable agreement in the variations of parameter α and wind speed, which indicates that the parameter α (Phillip's constant) represents wind effects on wave processes and is therefore geophysically real as suggested by Günther (1981). The parameter may be a measure of the spectral response to the wind forcing where wave generation is the active physical process. Although a significant correlation coefficient has been found between parameters α and f_m as may be seen in the later Fig 20, the agreement in the variations of f_m and wind speed is not remarkable as shown in Fig 18. In fact, the variations of γ and wind speed hardly agree as illustrated in Fig 19. Notice however, that the parameter γ is highly variable during the storm, which is consistent with the results from the simulation study.

During the second storm, similar results are obtained and presented in Figs 21, 22, 23 and 24, except the agreement in the variations of f_m and wind speed if found to be better in the second storm (Fig 22) than in the first storm (Fig 18). Also a significant correlation coefficient is found between parameters γ and σ_b as shown in Fig 24, which is consistent with the statistics of the JONSWAP parameters from the simulated spectra (see also Figs 8 and 9). The result emphasises the fact that the steeper the spectral tail, the great the departure between the JONSWAP and Pierson-Moskowitz spectral peaks.

It should be pointed out that in the simulation study, a significant correlation between parameters α and f_m is not found unlike during the first storm (see Fig 20). This is because there is no geophysical processes such as systematic wind forcing and wave generation involved in the simulation and so the values of α vary randomly and are uncorrelated with f_m values. However, when the geophysical processes are accounted for in the hourly spectra measured at Scilly Isles, the values of α grow systematically with the wind forcing. As the wave generation becomes active, the peak frequency f_m tends to shift toward the highest frequency end (see also Fig 12). Therefore, under both storm conditions, the α values seem to increase with the increase of f_m values, which provides a significant correlation as may be seen in Fig 20.

(vii) Predictability of Scilly Isles wave spectra

It has been noted that during the two storms, the amount of double-peaked spectra is approximately 24% of the total amount of spectra considered in the study. The main feature of a double-peaked spectrum is the partition of the energy about two distinct peak frequencies as can be seen in Fig 25 as well as in Figs 12 and 16. Probability distributions of the JONSWAP parameters α, f_m and γ illustrated respectively in Figs 27, 28, 29 for the first storm and Figs 30, 31, 32 for the second storm, generally show a bimodal distribution indicating the influence of the spectral double peaks. The bimodal distribution is most pronounced in the probability distributions of α (Figs 27 and 30). Although the distributions of f_m should also have a pronounced bimodal distribution as may be seen in the first storm (Fig 28), there seems to be no bimodal distribution of f_m in the second storm (Fig 31).

It is the double peaks in the wave spectra which cause possible inaccuracies in fitting the JONSWAP spectrum to the measured spectra. If these double-peaked spectra (approximately 24%) are removed from the total wave spectra, the rest of the spectra may provide reasonable fits with the JONSWAP spectrum. Thus, approximately 76% of the total spectra can be predicted using JONSWAP parametric prediction model, which is a relatively good predictability for Scilly Isles wave spectra. On the other hand, the predictability can be improved by improving the spectral fitting method to account for the spectral double peaks. Further discussion on the method will be made in the following section.

(viii) Recommendations

Soares (1984) presents a representation of double-peaked sea wave spectra. In his analysis, he recognises that a spectrum with two peaks often occurs whenever the sea state contains two wave systems such as a swell component with wind seas. He therefore, models the double-peaked spectra with two JONSWAP type of spectra. The approach is based on the assumption that a double-peaked spectrum is a sum of the swell and wind sea components. Similarly, the spectral moments can also be divided into the two components so that the sea state parameters such as H_s and T_z for each wave system or each spectral component can be estimated. Then, two parameters are used to compute the double-peaked JONSWAP spectrum with the three spectral parameters, γ, σ_a and σ_b fixed at their mean values. This promising approach also has the advantage of simplicity. Thus, it is recommended that the double-peaked spectra measured at Scilly Isles should be fitted by two JONSWAP type of spectra and a similar approach to Soares (1984) should be applied. Furthermore, a representation of a double-peaked spectrum by representing the swell component with the JONSWAP spectrum and the wind seas with the Pierson-Moskowitz spectrum, will provide an interesting experiment.

The application of JONSWAP spectrum to the single-peaked spectra of 80 degrees of freedom obtained from both the simulation and measurements at Scilly Isles, seems to indicate that the fitting procedure is adequate. There is no need for the further refined procedure to estimate the value of γ since the cause of the inaccurate value of γ is due to the relationship between ω_o and f_m (equation (6)) as discussed in section (iii) 'Results and discussion' on pages 4 and 6. The simulation study has also shown that the γ value is highly variable and is sensitive to the smoothness of a wave spectrum. Therefore, it is more important to improve the degrees of freedom in the wave measurements than the procedure to estimate γ via the maximum likelihood method.

Finally for some low energy spectra, it has been noted that the spectral noise level is relatively high as may be seen by the solid line in Fig 26. It is not certain whether the noise level is due to the instrumentation or the Fourier transform in the data analysis. However, the noise level must be further reduced to a lower level than in Fig 26.

4. ACKNOWLEDGEMENTS

The author wishes to thank Mr M J Tucker who made the opportunity to work on this project available, Mr Ray Gleason and Ms Mary T G Scott for their assistance on data acquisition and analysis. The author is grateful to her colleagues who helped to make her work at the IOS Taunton a pleasant experience.

The study was funded by the Department of Energy.

5. REFERENCES

GÜNTHER H, 1981. A Parametric Surface Wave Model and the Statistics of the Prediction Parameters (Hamburg: Max-Planck-Institut für Meteorologie)

HASSELMANN K, ROSS D B, MILLER P, and SELL W, 1976. J Phys Oceanogr, 6, (2), 200-228.

JENKINS G M and WATTS D G, 1968. Spectral Analysis and its Applications (San Francisco: Holden-Day)

LIU P C, 1983. Ocean Engng, 10 (6), 429-441

MOSKOWITZ L, 1964. J Geophys Res, 69 (24), 5161-5179.

PIERSON W J and MOSKOWITZ L, 1964. J Geophys Res, 69 (24), 5181-5189.

PIERSON W J, 1964. J Geophys Res, 69 (24), 5191-5203.

PIERSON W J, 1977. J Phys Oceanogr, 7, 127-134.

SOARES, C G, 1984. Ocean Engng, 11 (2), 185-208.

6. LIST OF TABLES AND FIGURES

Table 1 The means and variances of JONSWAP parameters obtained from fitting a JONSWAP spectrum to a simulated spectrum. There are 60 simulated spectra which were generated at 20,40 and 80 degrees of freedom.

Table 2 Correlation matrix of JONSWAP parameters, significant wave height H_s, zero crossing period T_z and the spectral band width obtained from 60 simulated wave spectra with 20 degrees of freedom.

Table 3 The same as Table 2 except for 40 degrees of freedom,

Table 4 The same as Table 2 except for 80 degrees of freedom,

Figure 1 Examples of simulated spectra shown by the dasked line compared with the fitted JONSWAP spectra plotted by dotted line. The mean JONSWAP spectrum is shown by the solid line and the simulation was carried out at 20 degrees of freedom.

Figure 2 The same as in Figure 1 except for 40 degrees of freedom.

Figure 3 The same as in Figure 1 except for 80 degrees of freedom.

Figure 4 The same as Figure 3 except the Pierson-Moskowitz spectrum was fitted instead of JONSWAP spectrum.

Figure 5 The JONSWAP parameter f_m is plotted against σ_a for zero means and 20 degrees of freedom.

Figure 6 The same as in Figure 5 except for 40 degrees of freedom.

Figure 7 The same as in Figure 5 except for 80 degrees of freedom.

Figure 8 The JONSWAP parameter γ is plotted against σ_b for zero means and 40 degrees of freedom.

Figure 9 The same as in Figure 8 except for 80 degrees of freedom,

Figure 10 The time series of H_s and power of the wave data recorded at the Isles of Scilly during the months of November and December 1981.

Figure 11 Example of the hourly wave spectra computed from the wave data recorded during the storm of 18-21 December 1981.

Figure 12 The same as in Figure 11 except during the storm of 25-28 December 1981.

Figure 13 The time series of wind speed (m s^{-1}) during the storm of 18-21 December 1981

Figure 14 The same as in Figure 13 except during the storm of 25-28 December 1981.

Figure 15 A comparison between the hourly spectra (in solid line) and the fitted JONSWAP spectra (in dashed line) during the first storm.

Figure 16 The same as in Figure 15 except during the second storm.

Figure 17 A comparison between the time series of JONSWAP parameter α and the time series of wind speed during the first storm.

Figures continued:

Figure 18 The same as in Figure 17 except for parameter f_m.

Figure 19 The same as in Figure 17 except for parameter γ

Figure 20 The parameter α is plotted against parameter f_m to indicate the correlation between the two parameters during the first storm.

Figure 21 The same as in Figure 17 except during the second storm.

Figure 22 The same as in Figure 18 except during the second storm.

Figure 23 The same as in Figure 19 except during the second stormm.

Figure 24 The parameter γ is plotted against parameter σ_b to indicate the correlation between the two parameters during the second storm.

Figure 25 Examples of double-peaked spectra obtained at Scilly Isles during both storms.

Figure 26 A comparison between a double-peaked spectrum (in solid line) and the fitted JONSWAP spectrum (in dashed line) indicating the unsatisfactory results.

Figure 27 A probability distribution of parameter α during the first storm,

Figure 28 A probability distribution of parameter f_m during the first storm,

Figure 29 A probability distribution of parameter γ during the first storm,

Figure 30 The same as in Figure 27 except during the second storm,

Figure 31 The same as in Figure 28 except during the second storm.

Figure 32 The same as in Figure 29 except during the second storm.

TABLE 1: The means and variances of JONSWAP parameters obtained from fitting a JONSWAP spectrum to a simulated spectrum. Sixty simulated spectra were generated at 20, 40 and 80 degrees of freedom. A value in the bracket is a percentage of the variance changing due to the increase in degrees of freedom.

JONSWAP Parameters	True Value	20 degrees of freedom		40 degrees of freedom		80 degrees of freed	
		Mean	Variance	Mean	Variance	Mean	Variance
α	0.0162	0.0154	$.1647 \times 10^{-5}$	0.0158	$.1069 \times 10^{-5}$ (35.09%)	0.0161	$.3905 \times 10^{-6}$ (76.29%)
f_m	0.364	0.3639	$.1211 \times 10^{-2}$	0.3609	$.9218 \times 10^{-4}$ (23.88%)	0.3641	$.5708 \times 10^{-4}$ (52.86%)
γ	3.3	4.4618	1.4740	3.9874	.6603 (55.20%)	3.8372	.3510 (76.19%)
σ_a	0.07	0.0563	$.1899 \times 10^{-2}$	0.0474	$.1111 \times 10^{-2}$ (41.50%)	0.0633	$.1074 \times 10^{-2}$ (43.44%)
σ_b	0.09	0.0707	$.1036 \times 10^{-2}$	0.0840	$.1170 \times 10^{-2}$ (12.93%)	0.0790	$.5631 \times 10^{-3}$ (45.65%)

Table 2 Correlation matrix of JONSWAP parameters, significant wave height HS, zero crossing period TZ, and spectral band width SBW obtained from 60 simulated wave spectra with 20 degrees of freedom.

	ALPHA	FM	GAMMA	SIGMA-A	SIGMA-B	HS	TZ	SBW
ALPHA	1.0000							
FM	0.2854	1.0000						
GAMMA	-0.1269	0.4591	1.0000					
SIGMA-A	0.1699	**0.8423**	0.0876	1.0000				
SIGMA-B	-0.3084	-0.5675	-0.5861	-0.2804	1.0000			
HS	0.2559	-0.0264	0.3316	-0.0950	0.1738	1.0000		
TZ	-0.4579	-0.0815	0.4581	-0.0790	0.1828	0.5009	1.0000	
SBW	0.2380	-0.1527	-0.5567	-0.0199	-0.1131	-0.6280	-0.4871	1.0000

Table 3 Correlation matrix of JONSWAP parameters, significant wave height HS, zero crossing period TZ, and spectral band width SBW obtained from 60 simulated wave spectra with 40 degrees of freedom.

	ALPHA	FM	GAMMA	SIGMA-A	SIGMA-B	HS	TZ	SBW
ALPHA	1.0000							
FM	0.3378	1.0000						
GAMMA	-0.0114	0.6612	1.0000					
SIGMA-A	0.2819	0.8967	0.4760	1.0000				
SIGMA-B	-0.4564	-0.8354	-0.7694	-0.6763	1.0000			
HS	0.2258	-0.0689	0.2463	0.0128	-0.0204	1.0000		
TZ	-0.4357	-0.1104	0.3892	0.0178	0.0113	0.4240	1.0000	
SBW	0.5326	-0.0944	-0.4247	-0.0770	-0.0997	-0.3851	-0.3744	1.0000

Table 4 Correlation matrix of JONSWAP parameters, significant wave height HS, zero crossing period TZ, and spectral band width SBW obtained from 60 simulated wave spectra with 80 degrees of freedom.

	ALPHA	FM	GAMMA	SIGMA-A	SIGMA-B	HS	TZ	SBW
ALPHA	1.0000							
FM	0.4249	1.0000						
GAMMA	-0.0150	0.5227	1.0000					
SIGMA-A	0.3098	0.8892	0.2519	1.0000				
SIGMA-B	-0.4030	-0.7094	-0.7176	-0.4671	1.0000			
HS	-0.0250	-0.0006	0.1690	-0.0029	-0.0020	1.0000		
TZ	-0.0465	-0.0003	0.1269	-0.0230	-0.0536	0.9755	1.0000	
SBW	0.0599	-0.0130	-0.1620	0.0105	0.0256	-0.9876	-0.9938	1.0000

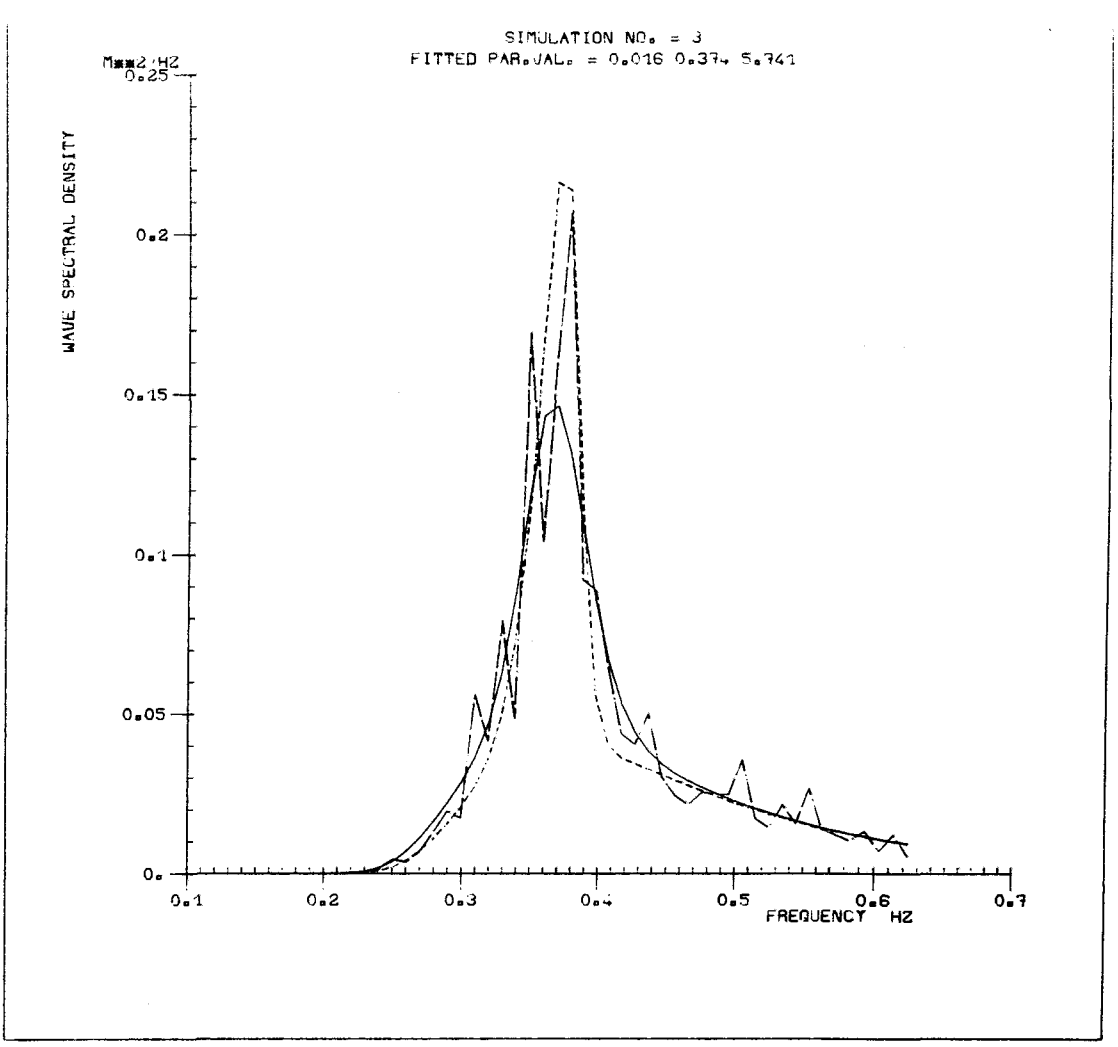
SIMULATION NO. = 3
FITTED PAR.VAL. = 0.016 0.374 5.741
M**2/HZ
WAVE SPECTRAL DENSITY
0.25
0.2
0.15
0.1
0.05
0.
0.1
0.2
0.3
0.4
0.5
0.6
0.7
FREQUENCY HZ

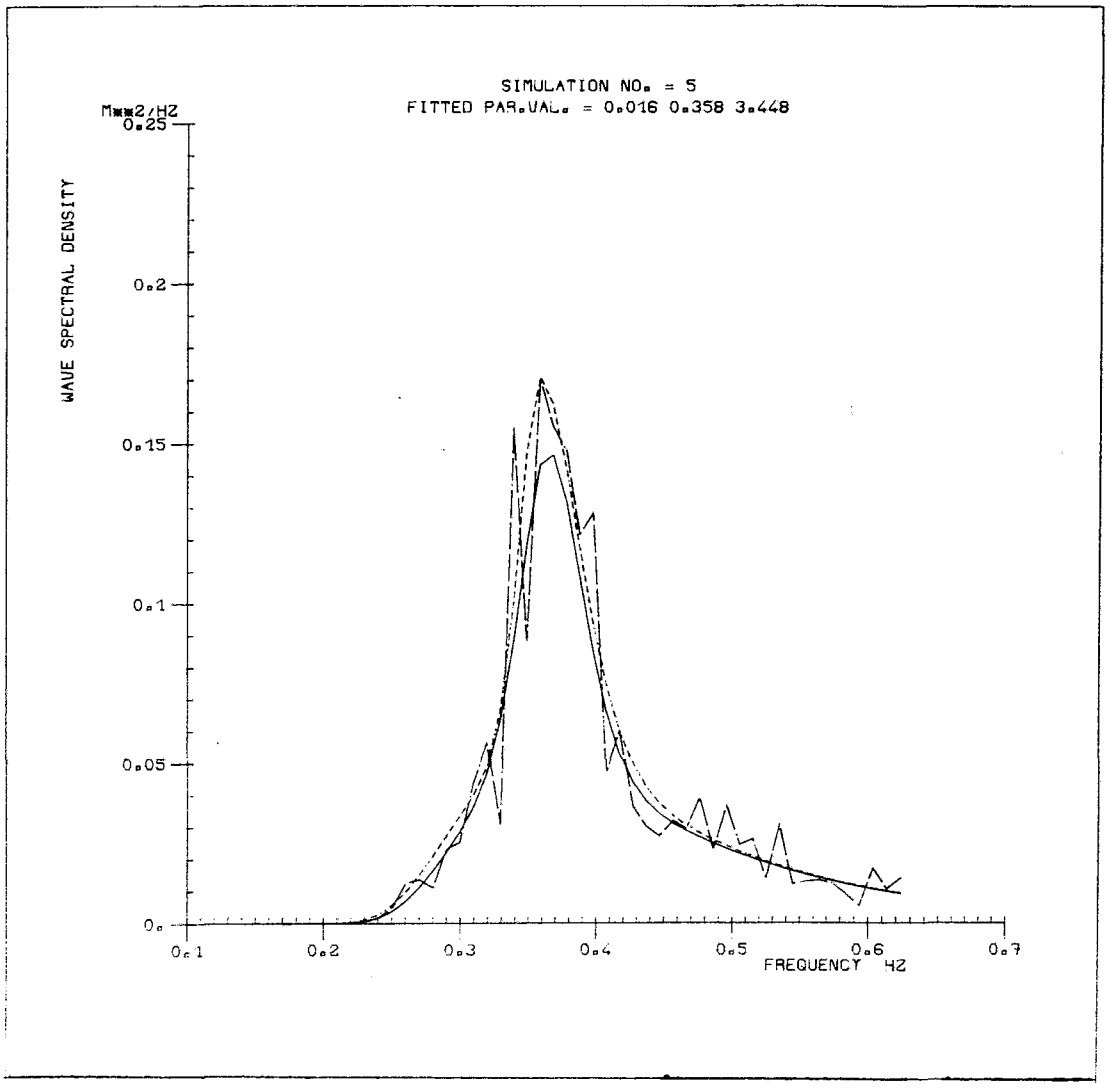
SIMULATION NO. = 5
FITTED PAR.VAL. = 0.016 0.358 3.448
M**2/HZ
WAVE SPECTRAL DENSITY
0.25
0.2
0.15
0.1
0.05
0.
0.1
0.2
0.3
0.4
0.5
0.6
0.7
FREQUENCY HZ

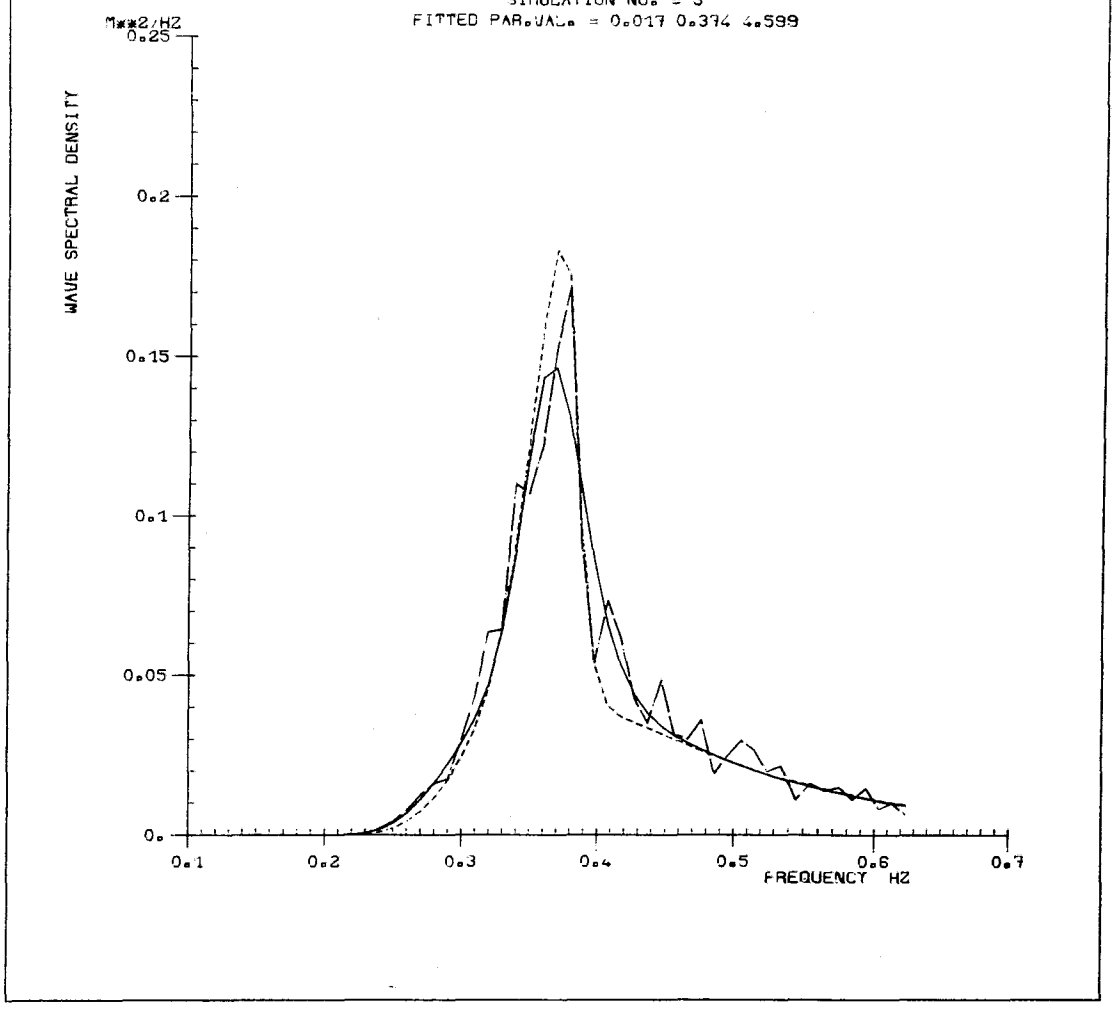
SIMULATION NO. = 3
FITTED PAR.VAL. = 0.017 0.394 4.599
M**2/HZ
WAVE SPECTRAL DENSITY
0.25
0.2
0.15
0.1
0.05
0.
0.1
0.2
0.3
0.4
0.5
0.6
0.7
FREQUENCY HZ

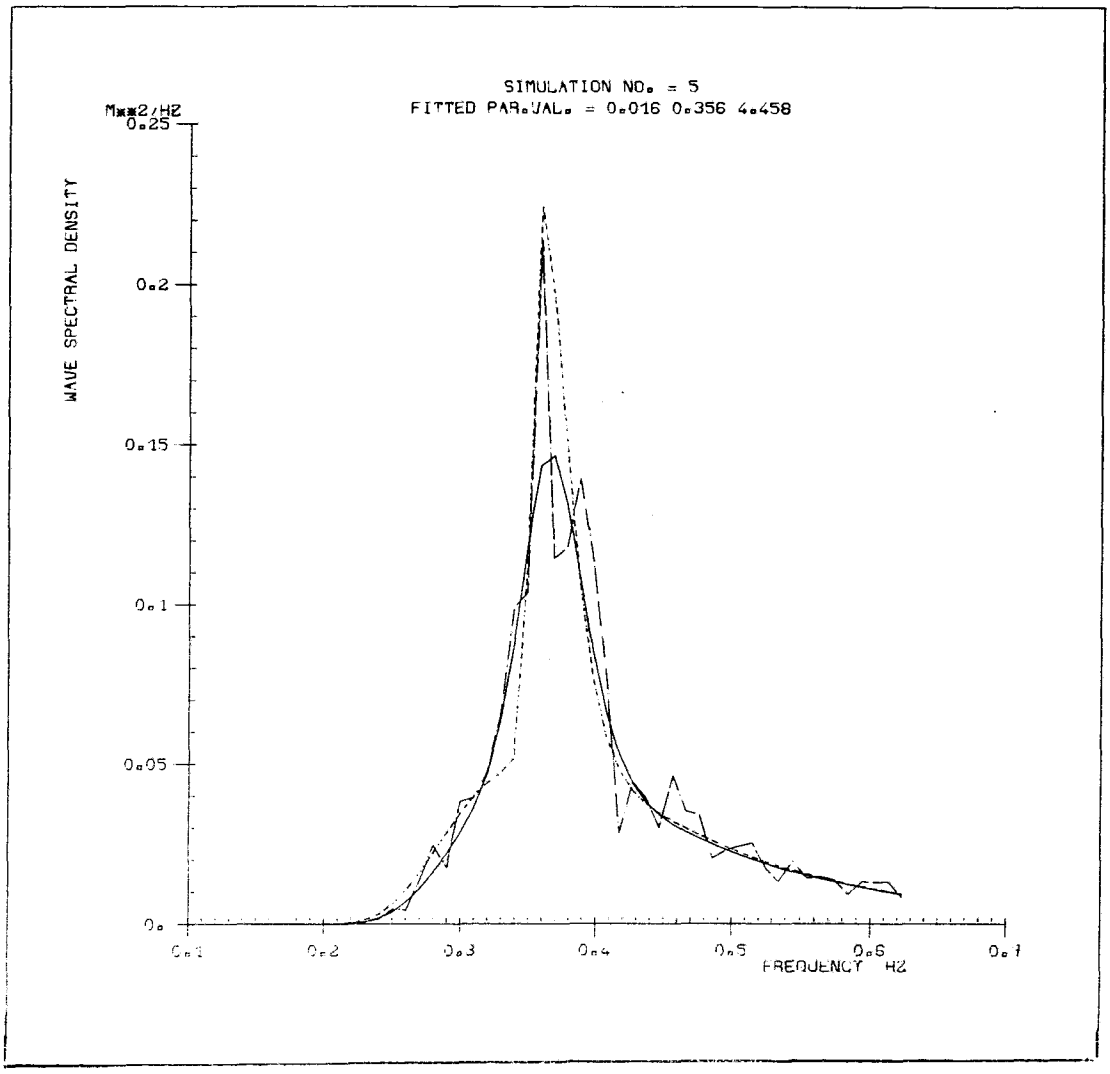
SIMULATION NO. = 5
FITTED PAR.VAL. = 0.016 0.356 4.458
M**2/HZ
WAVE SPECTRAL DENSITY
0.25
0.2
0.15
0.1
0.05
0.
0.1
0.2
0.3
0.4
0.5
0.6
0.7
FREQUENCY HZ

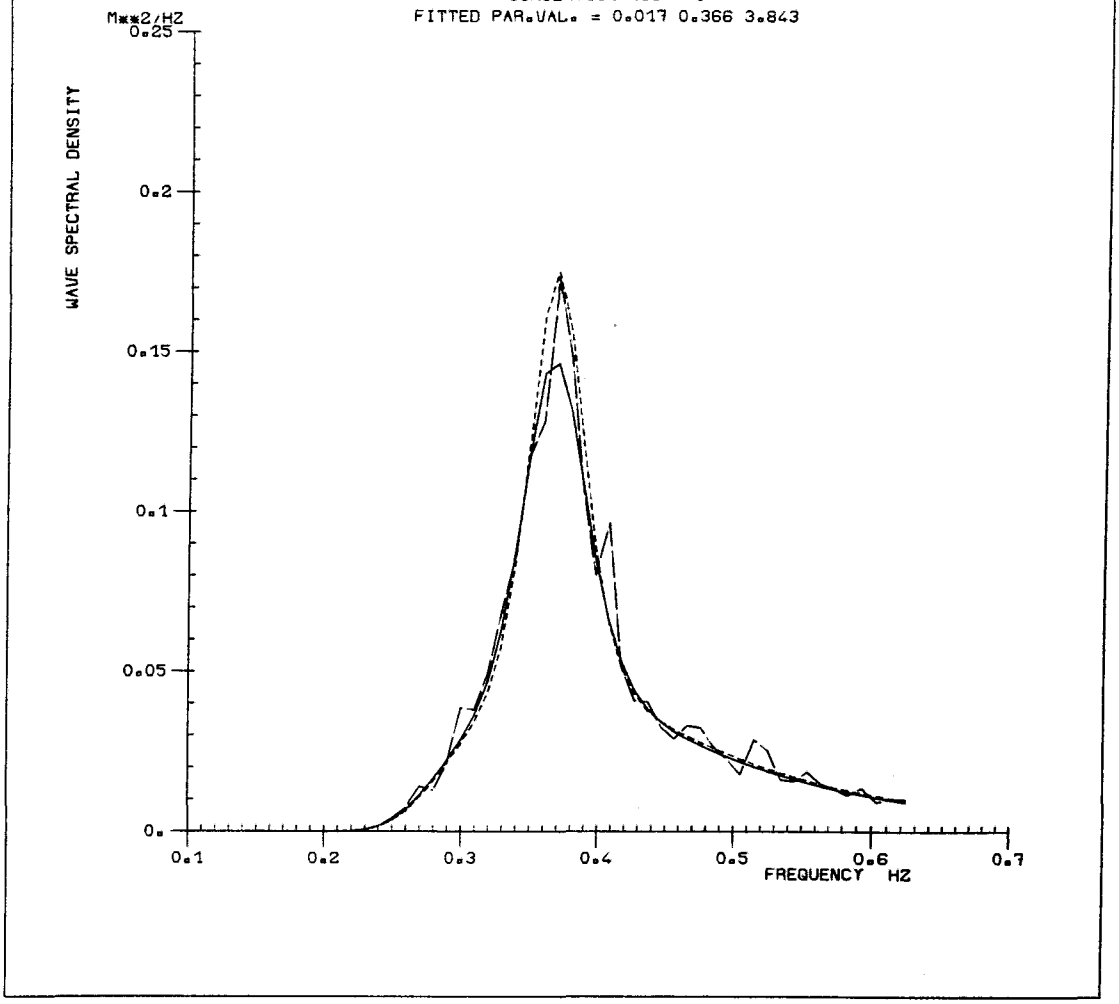
SIMULATION NO. = 3
FITTED PAR.VAL. = 0.017 0.366 3.843
M**2/HZ
WAVE SPECTRAL DENSITY
0.25
0.2
0.15
0.1
0.05
0.
0.1
0.2
0.3
0.4
0.5
0.6
0.7
FREQUENCY HZ

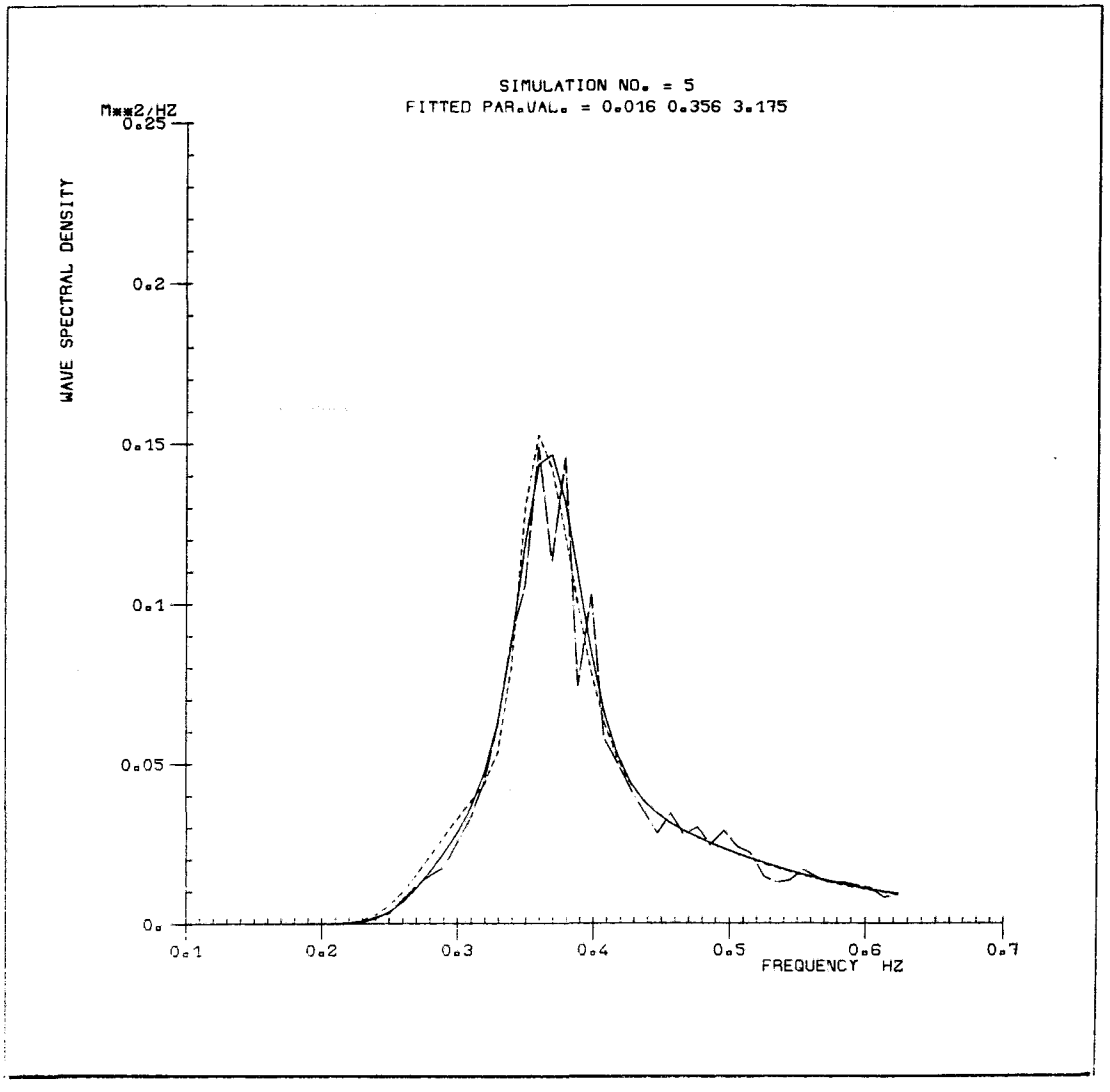
SIMULATION NO. = 5
FITTED PAR.VAL. = 0.016 0.356 3.175
M**2/HZ
WAVE SPECTRAL DENSITY
0.25
0.2
0.15
0.1
0.05
0.
0.1
0.2
0.3
0.4
0.5
0.6
0.7
FREQUENCY HZ

Fig. 4

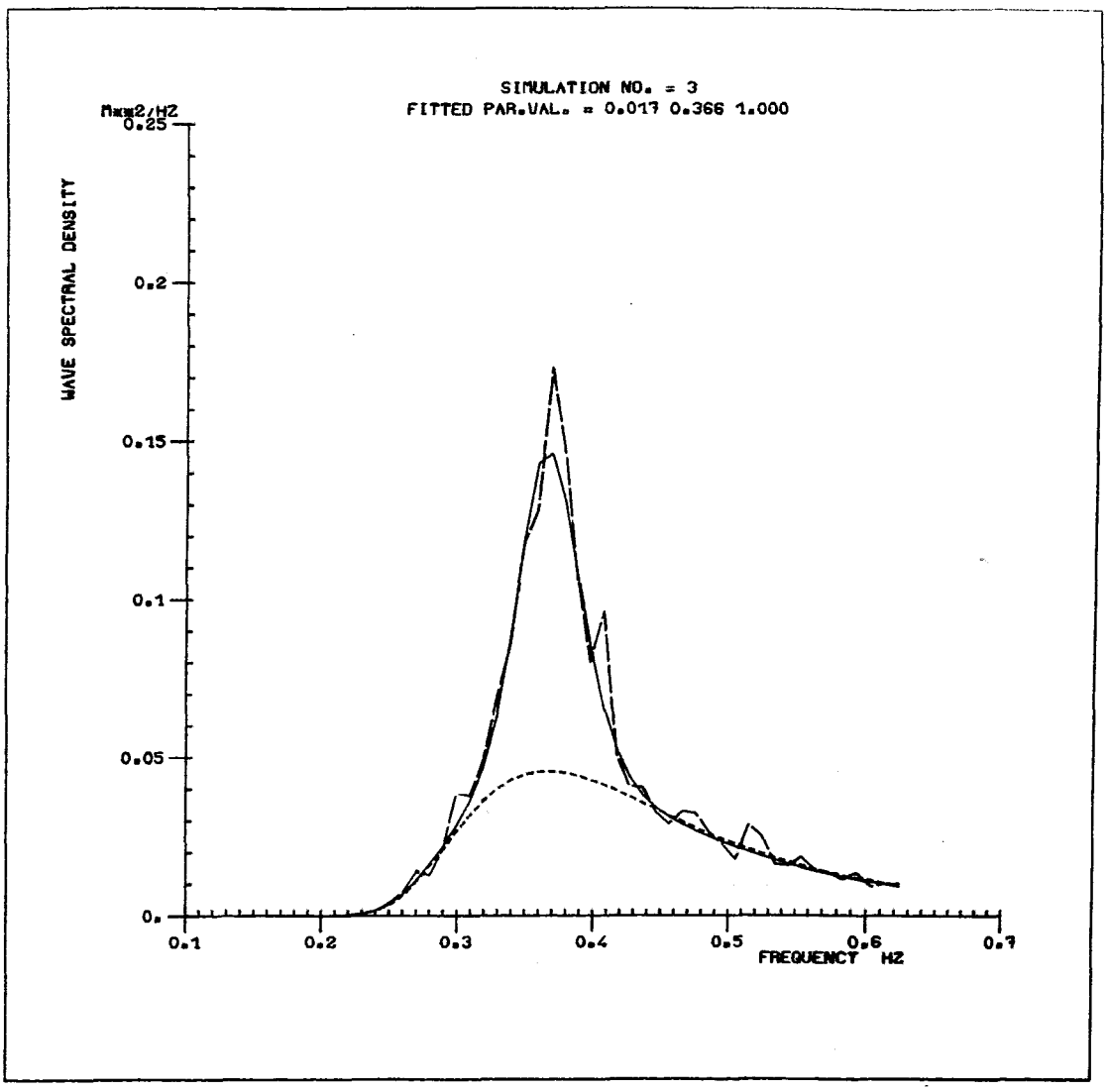
SIMULATION NO. = 3
FITTED PAR.VAL. = 0.017 0.366 1.000
M**2/HZ
WAVE SPECTRAL DENSITY
0.25
0.2
0.15
0.1
0.05
0.
0.1
0.2
0.3
0.4
0.5
0.6
0.7
FREQUENCY HZ

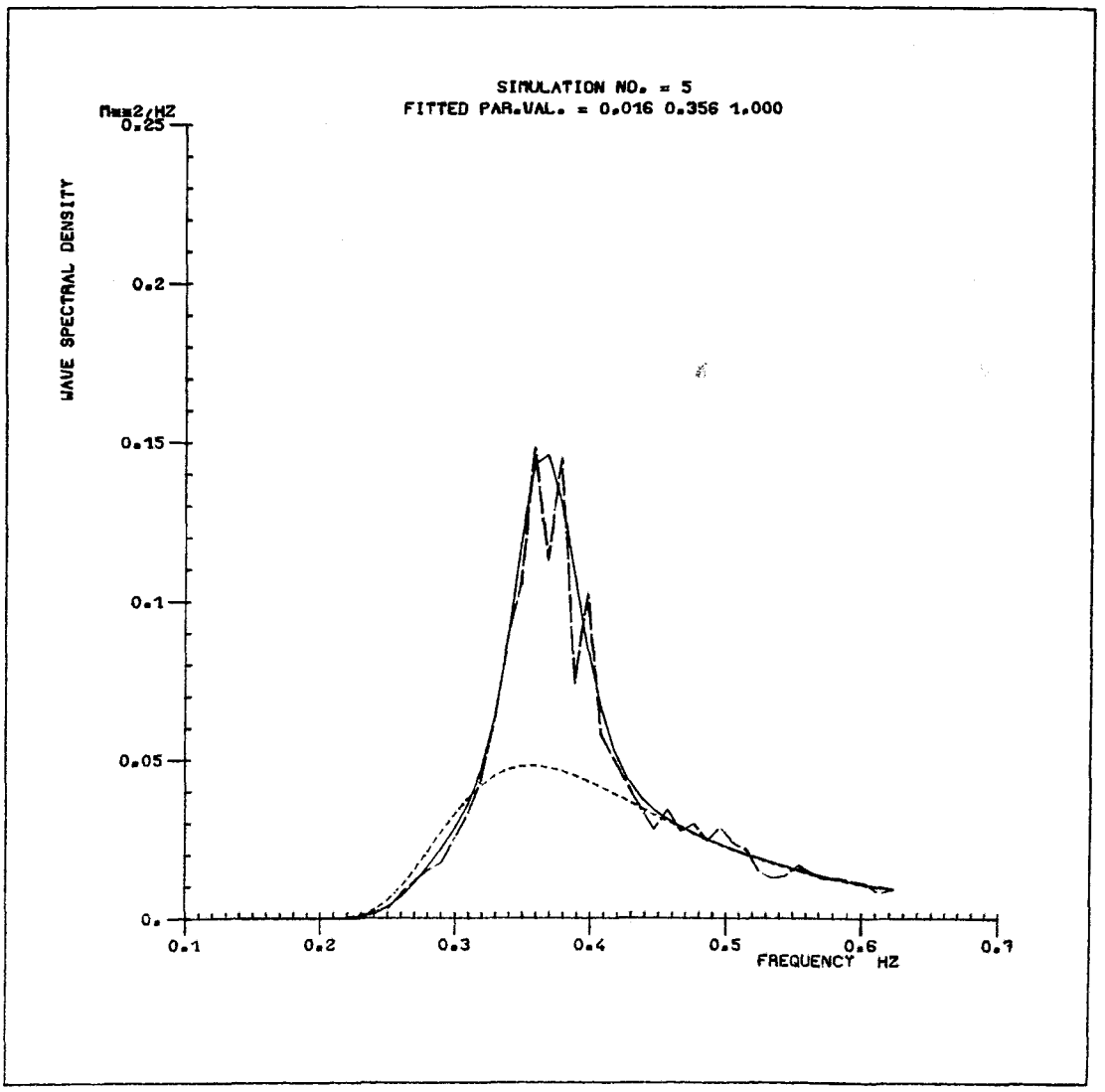
SIMULATION NO. = 5
FITTED PAR.VAL. = 0.016 0.356 1.000
M**2/HZ
WAVE SPECTRAL DENSITY
0.25
0.2
0.15
0.1
0.05
0.
0.1
0.2
0.3
0.4
0.5
0.6
0.7
FREQUENCY HZ

Fig. 5

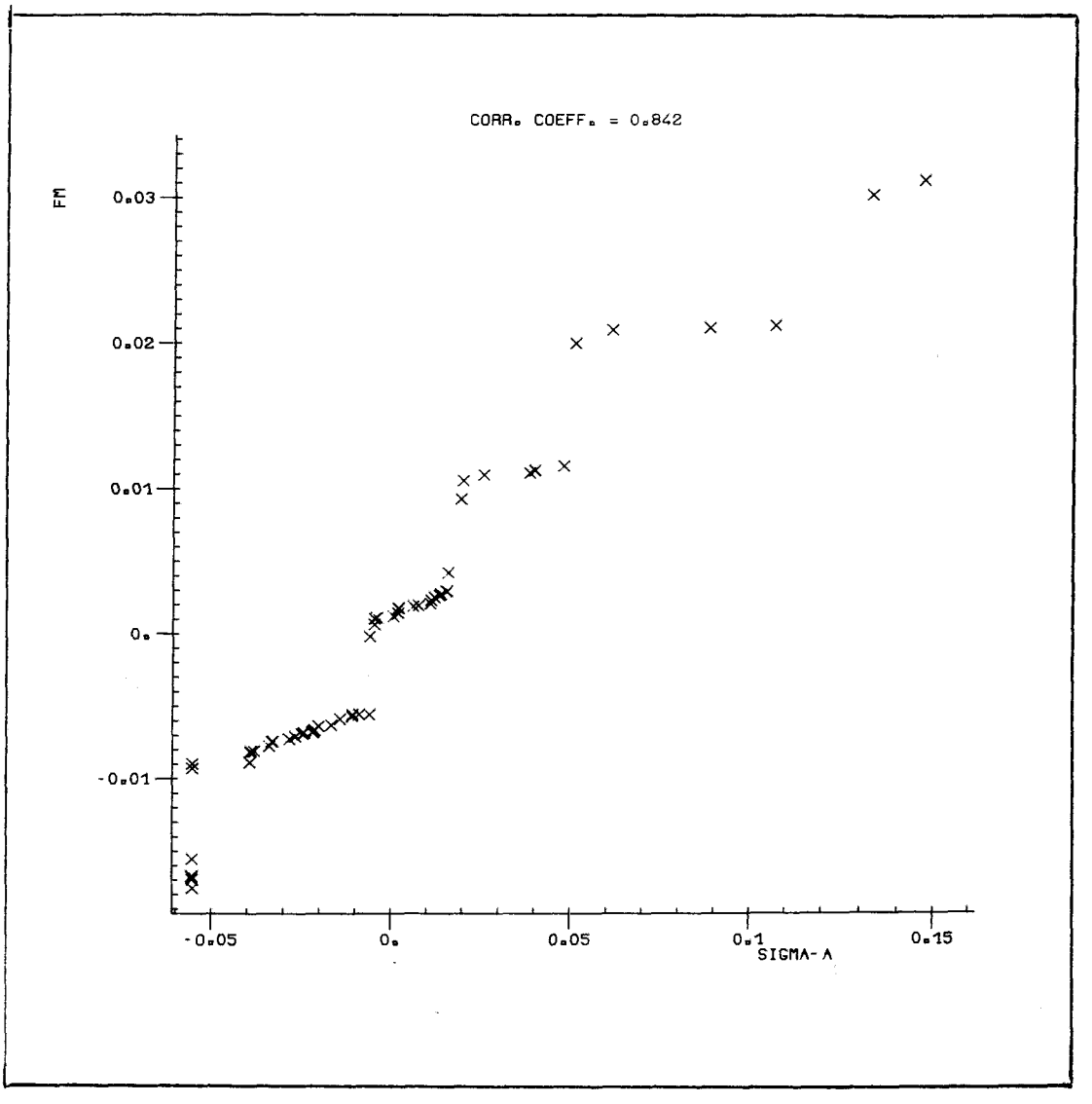

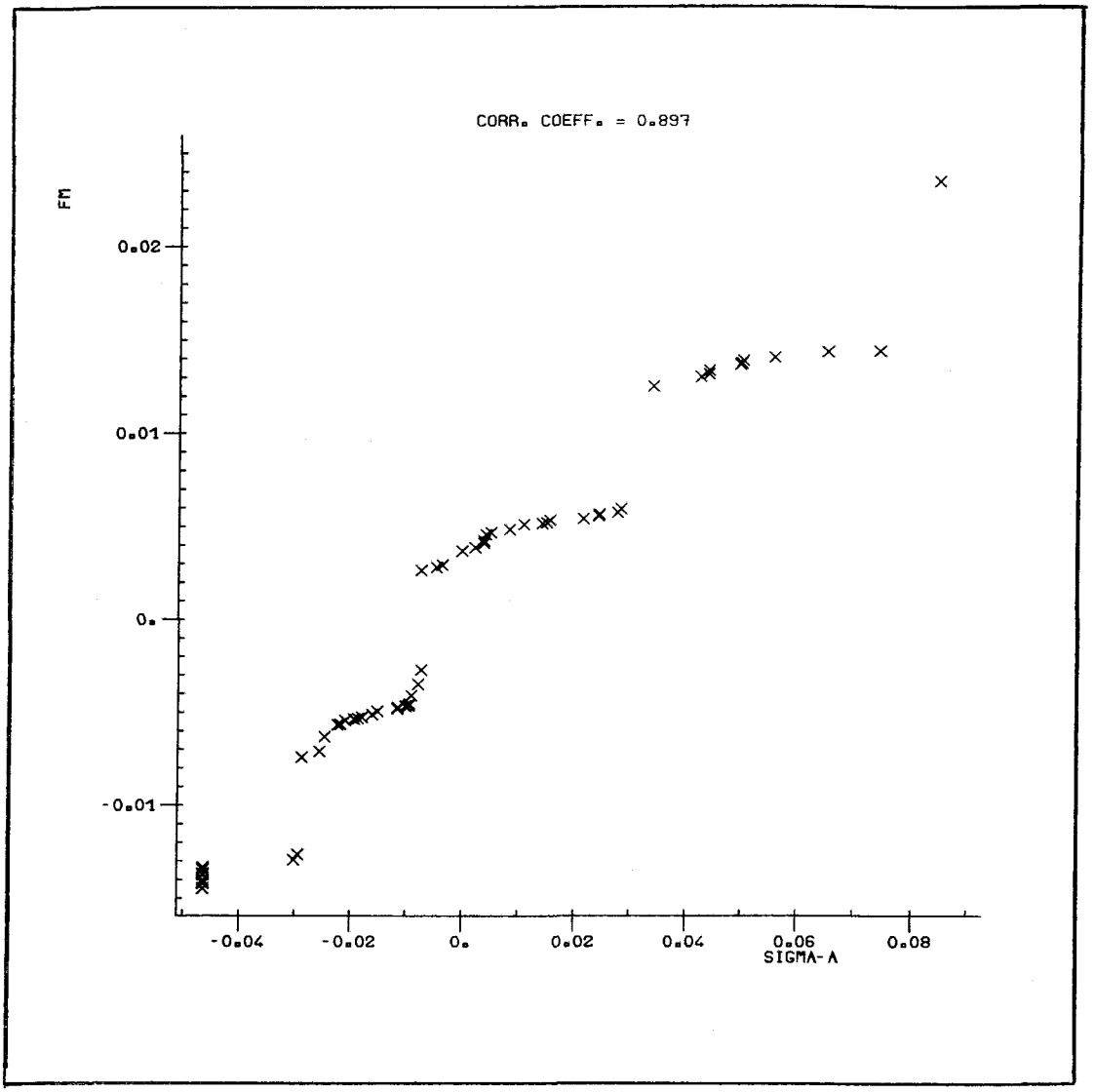
CORR. COEFF. = 0.897
FM
0.02
0.01
0.
-0.01
-0.04
-0.02
0.
0.02
0.04
0.06
0.08
SIGMA-A

Fig. 7

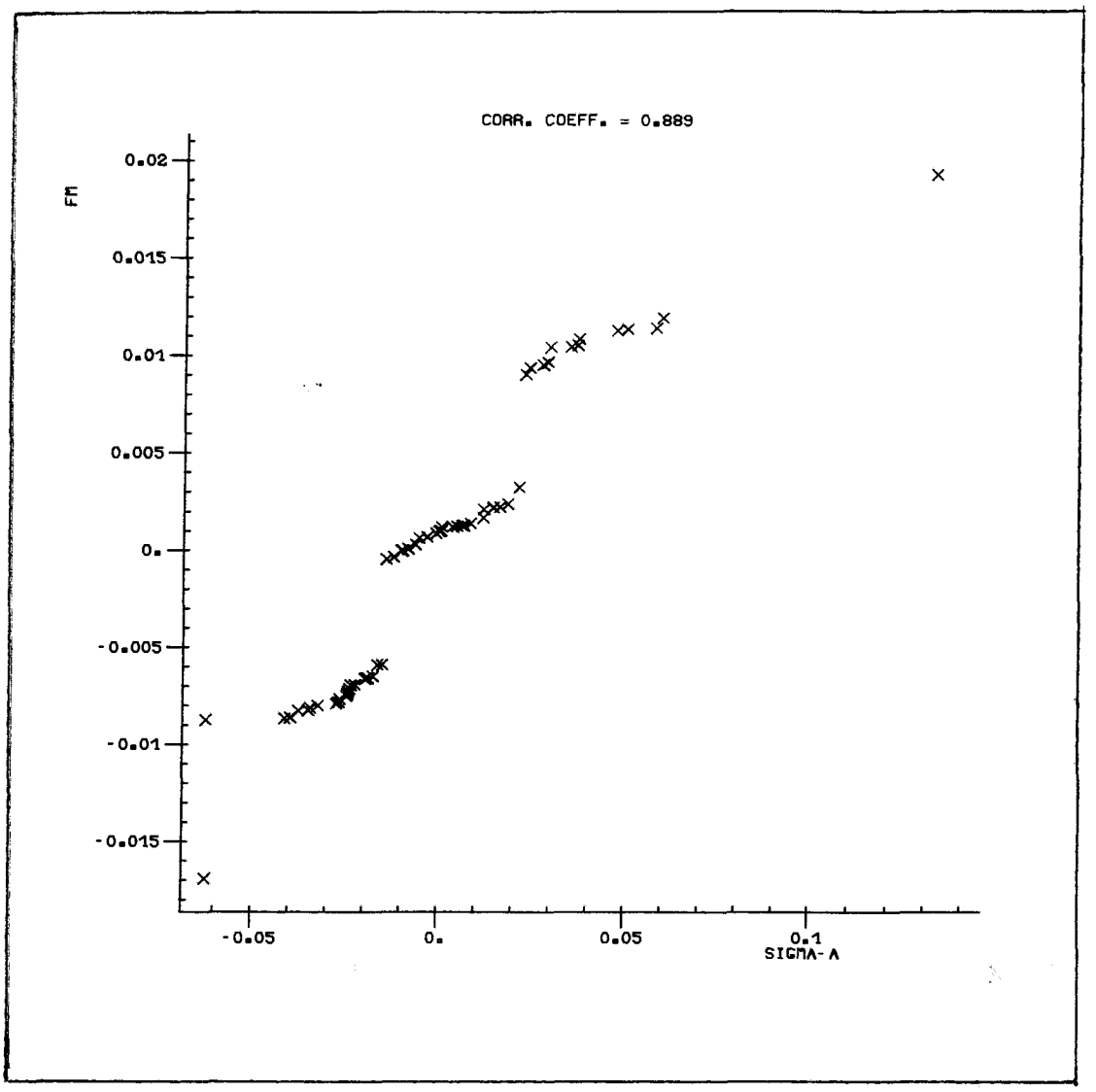
CORR. COEFF. = 0.889
FM
0.02
0.015
0.01
0.005
0.
-0.005
-0.01
-0.015
-0.05
0.
0.05
0.1
SIGMA-A

Fig. 8

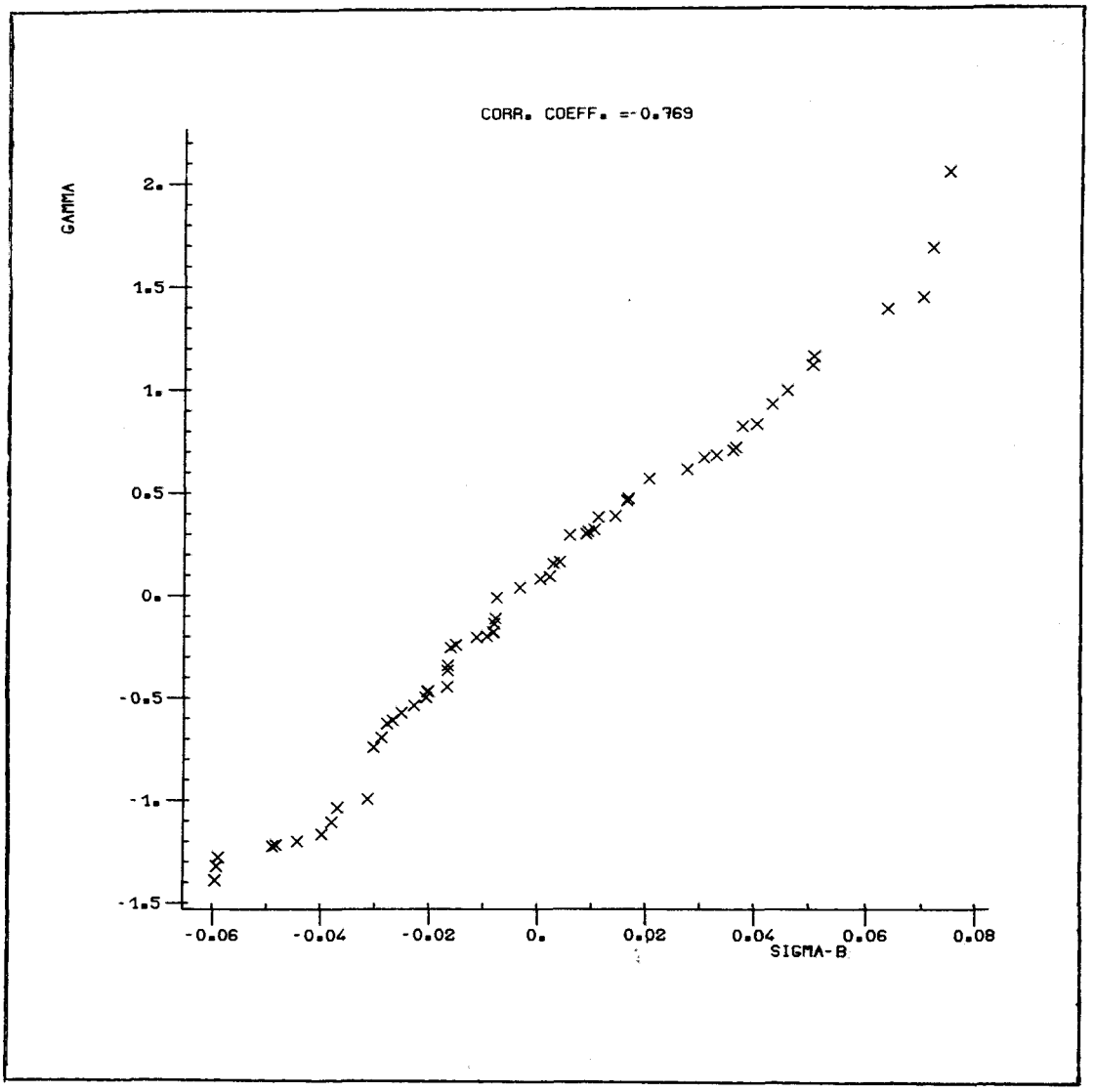
CORR. COEFF. =-0.769
GAMMA
2.
1.5
1.
0.5
0.
-0.5
-1.
-1.5
-0.06
-0.04
-0.02
0.
0.02
0.04
0.06
0.08
SIGMA-B

Fig. 9

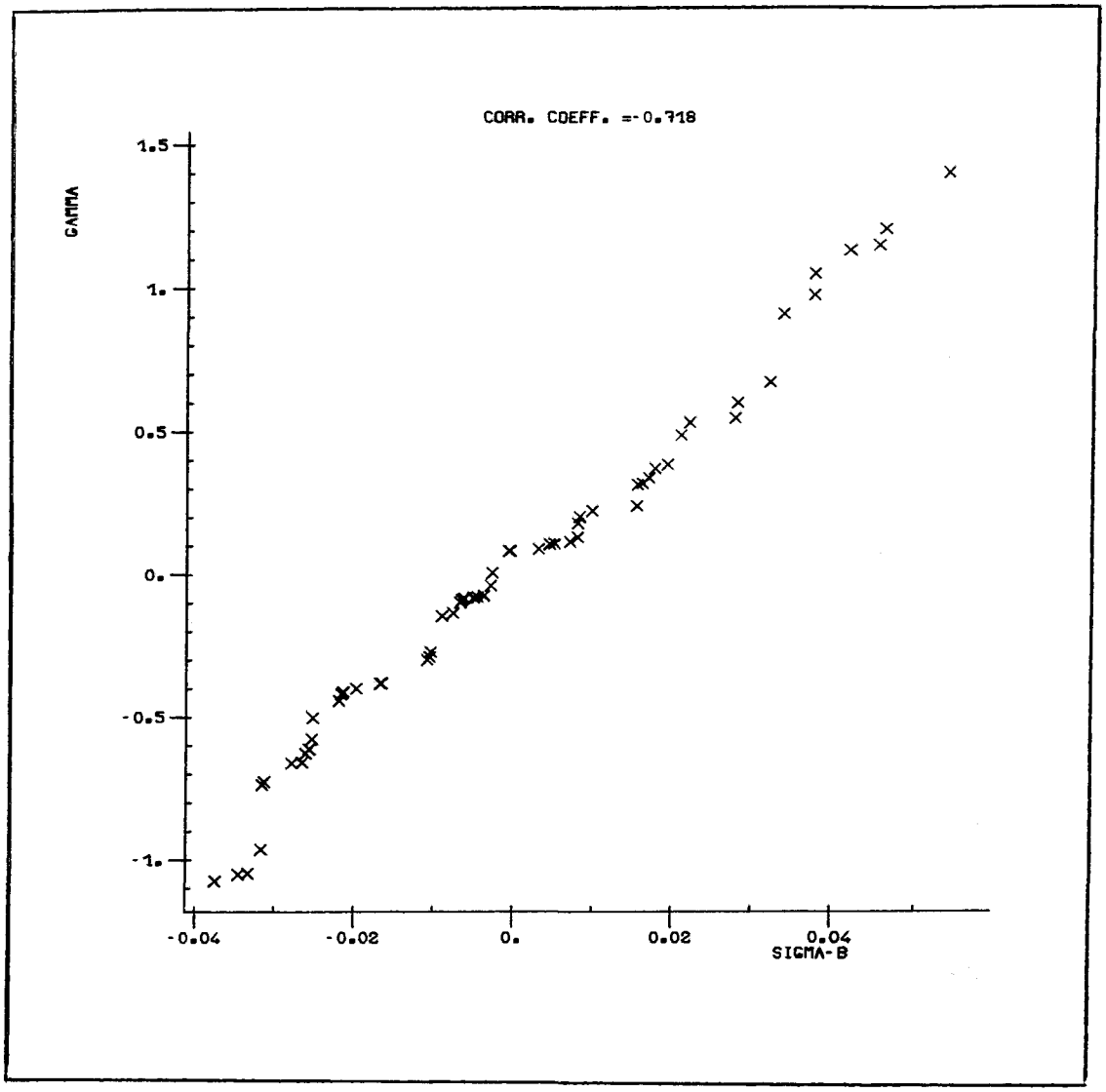

TIME SERIES OF Hs

ISLES OF SCILLY WAVERIDER

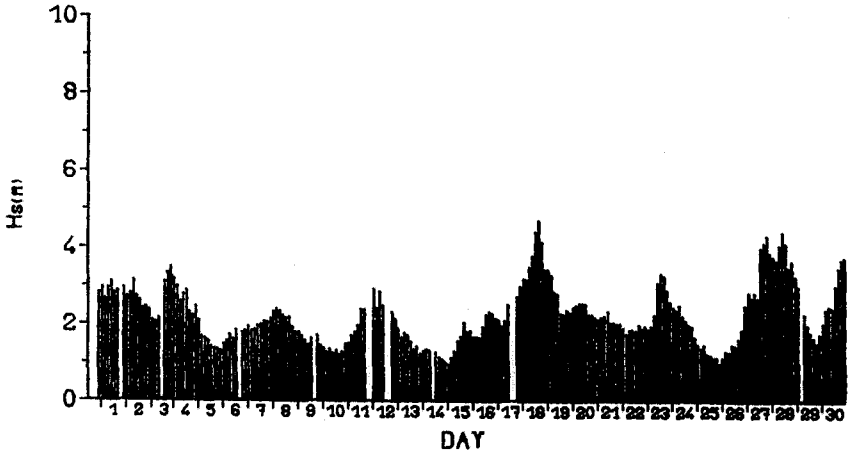

NOV 1981

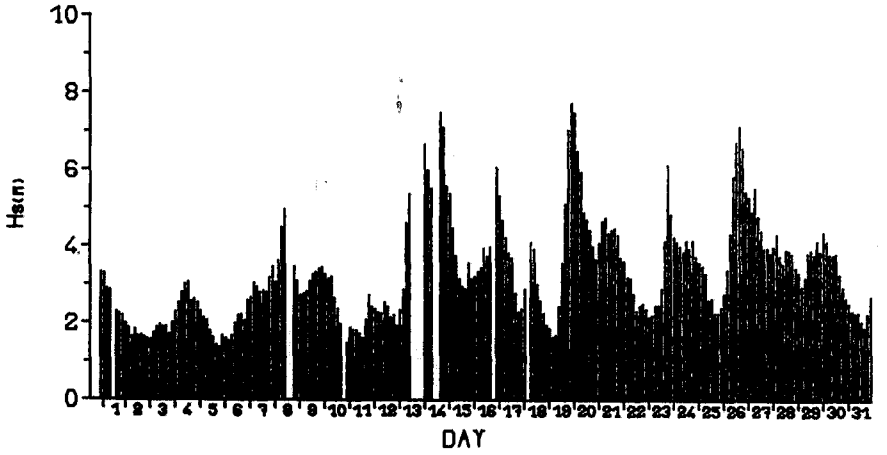

DEC 1981

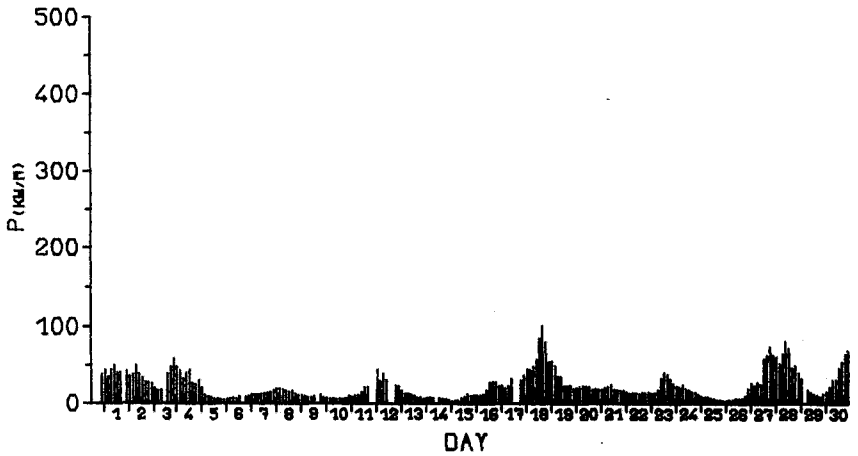

NOV 1981

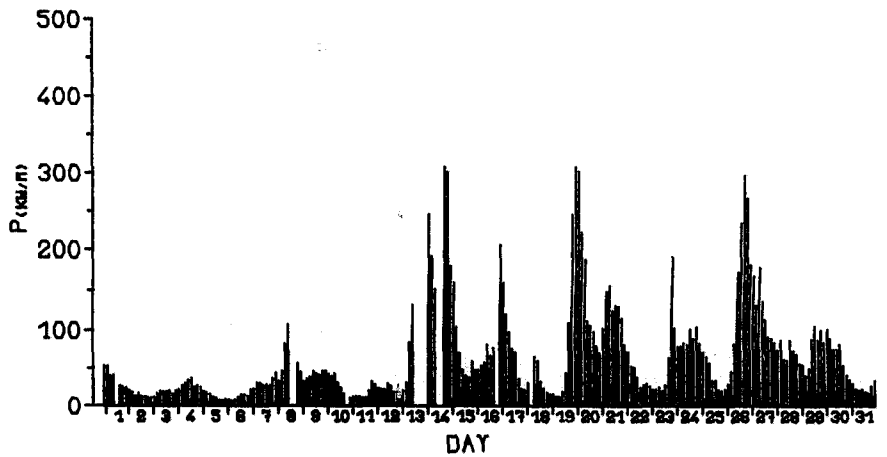

DEC 1981

TIME SERIES OF POWER

ISLES OF SCILLY WAVERIDER

Fig. 11

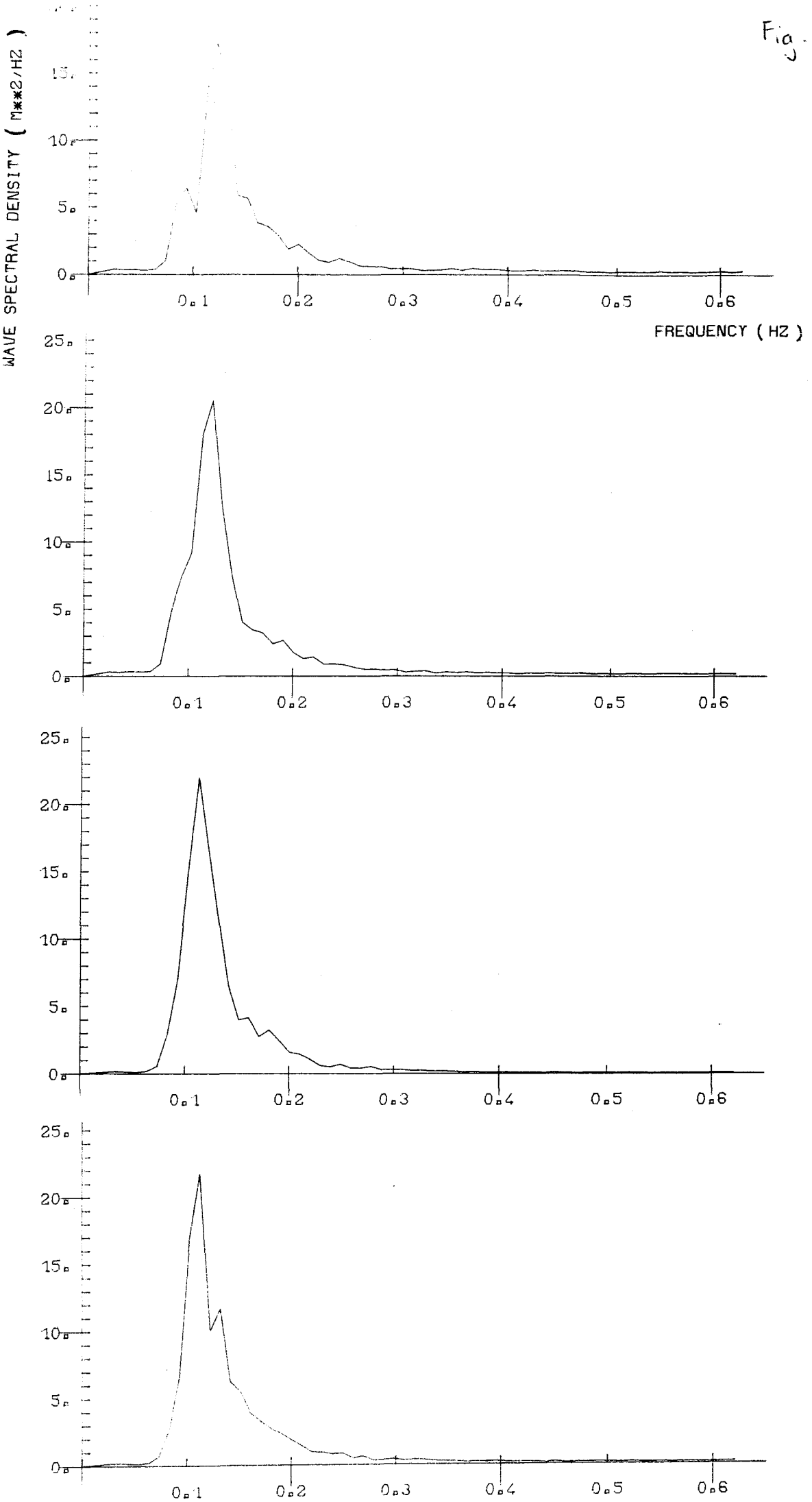
WAVE SPECTRAL DENSITY (M**2/HZ)
FREQUENCY (HZ)
0.1
0.2
0.3
0.4
0.5
0.6
5.
10.
15.
20.
25.
0.

Fig. 12

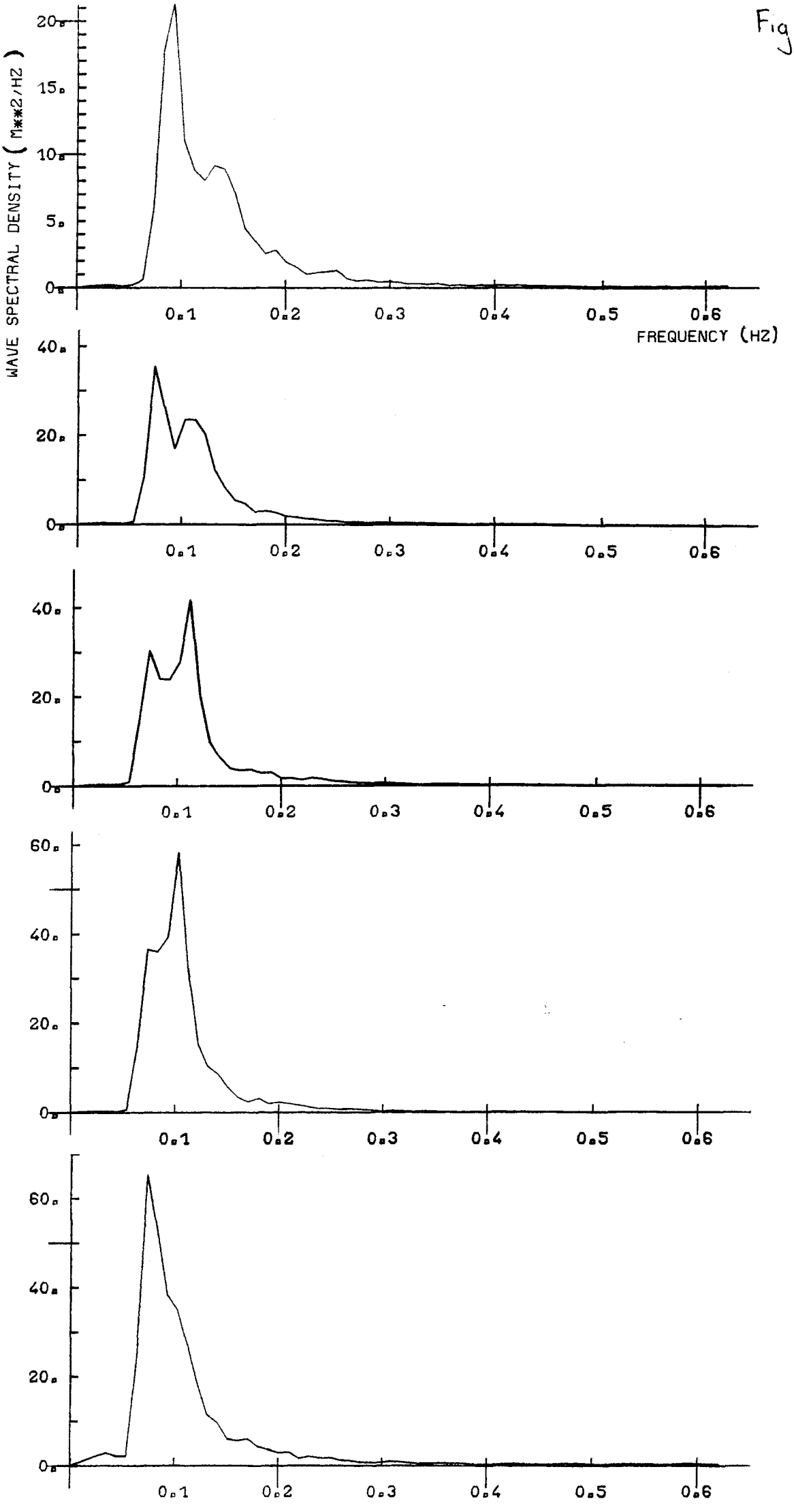
WAVE SPECTRAL DENSITY (M**2/HZ)
20.
15.
10.
5.
0.
0.1
0.2
0.3
0.4
0.5
0.6
FREQUENCY (HZ)
40.
20.
0.
60.

Fig. 13

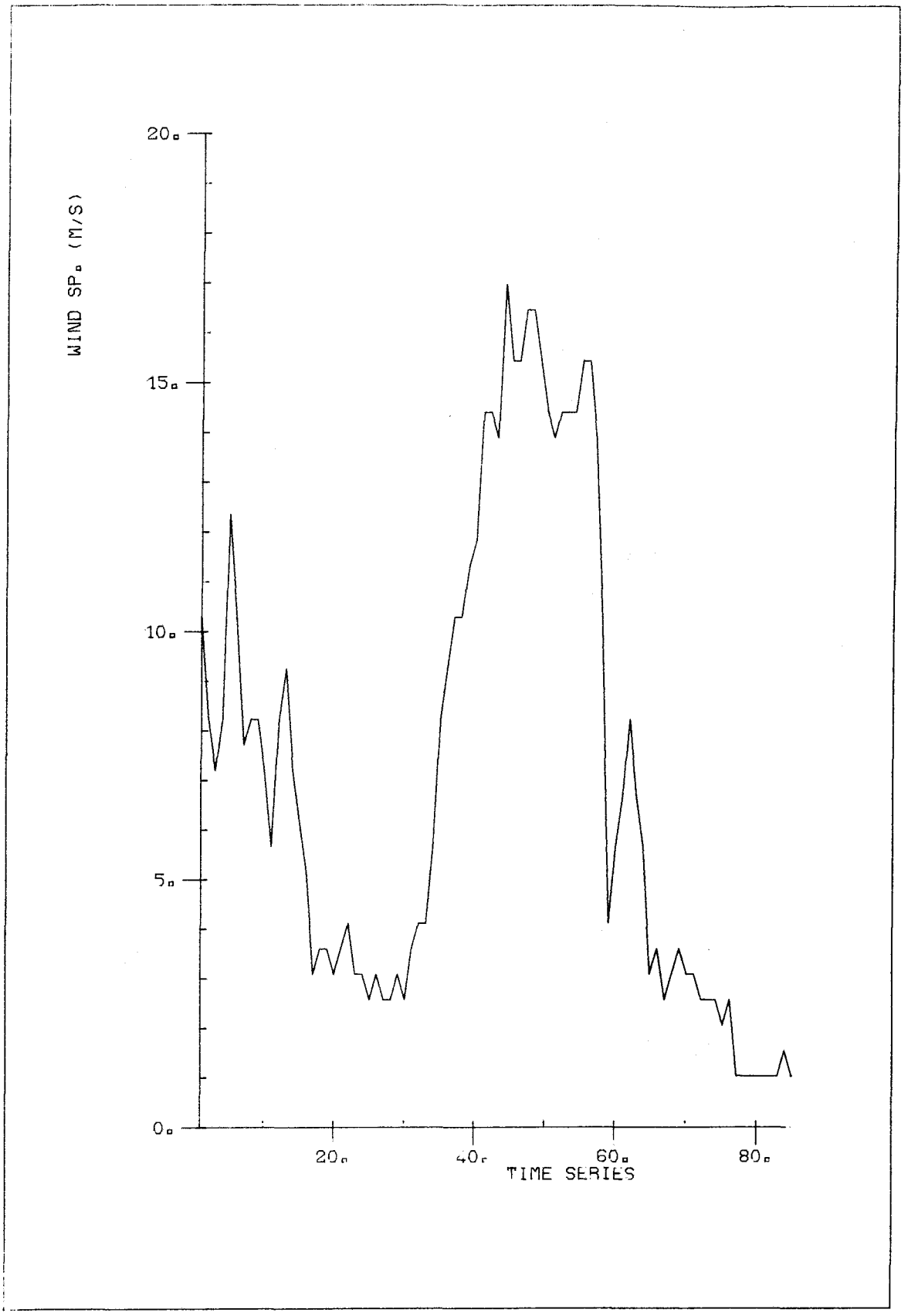

Fig. 11

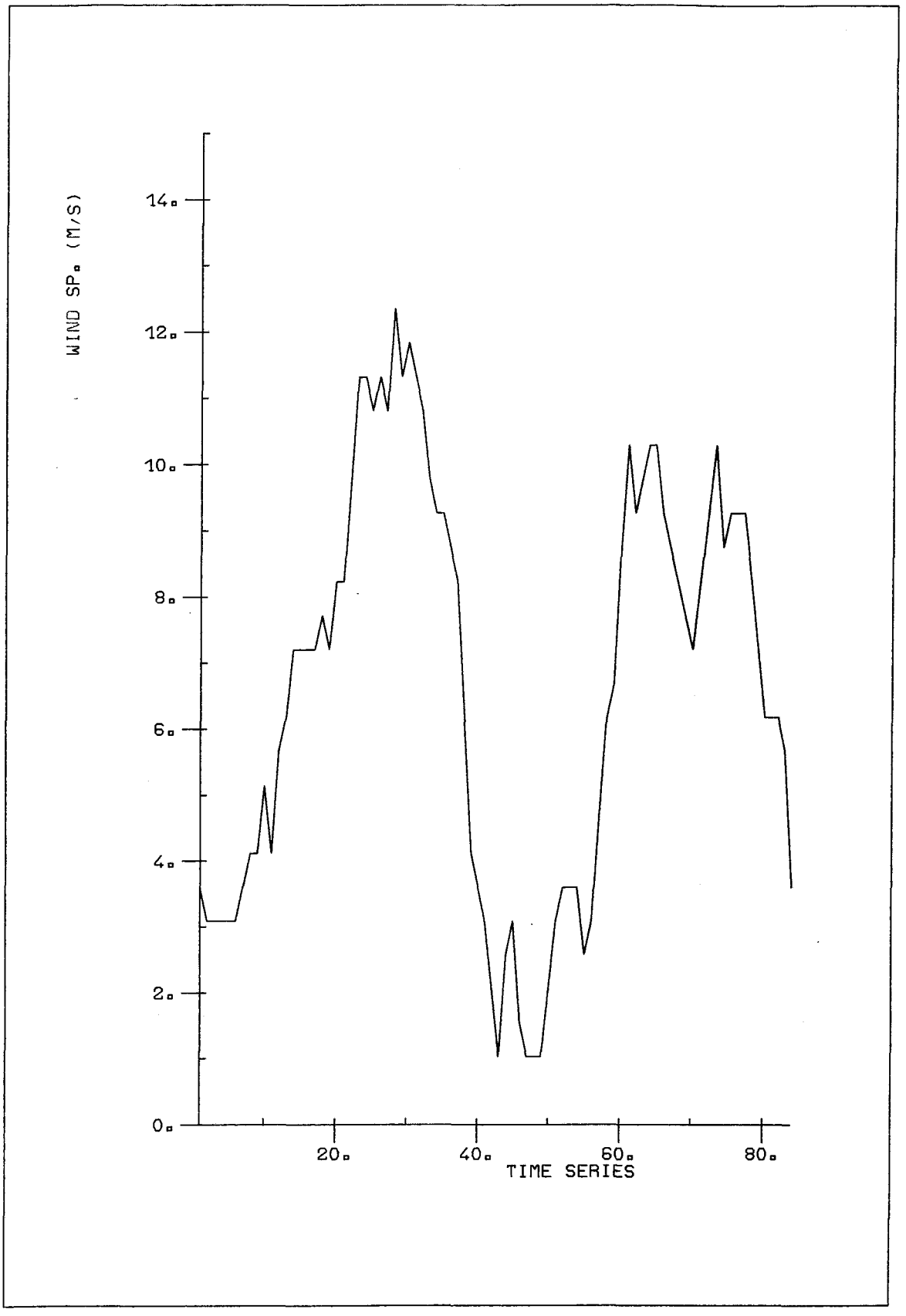

Fig. 15

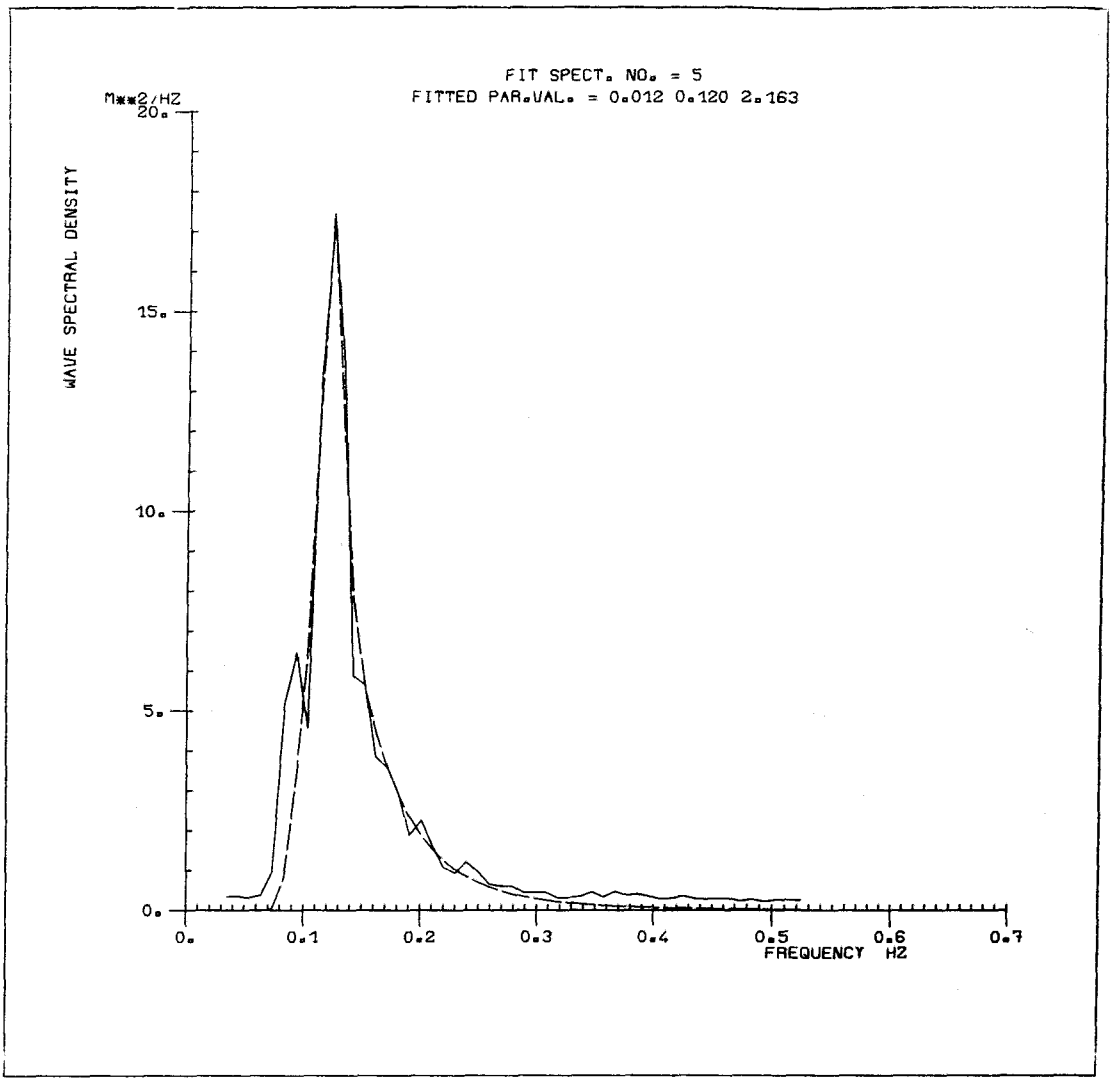
FIT SPECT. NO. = 5
FITTED PAR.VAL. = 0.012 0.120 2.163
M**2/HZ
WAVE SPECTRAL DENSITY
20.
15.
10.
5.
0.
0.
0.1
0.2
0.3
0.4
0.5
0.6
0.7
FREQUENCY HZ

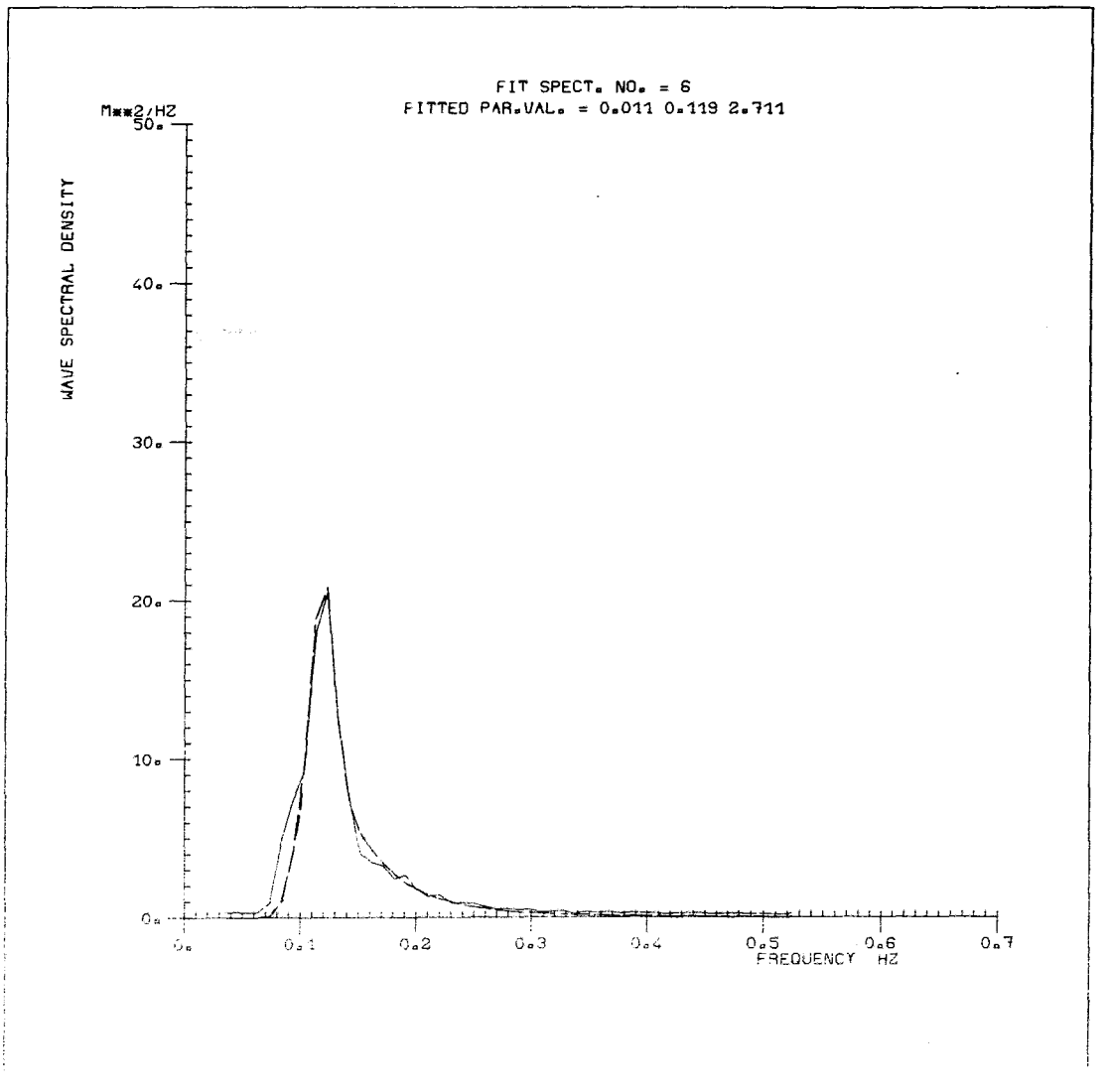
FIT SPECT. NO. = 6
FITTED PAR.VAL. = 0.011 0.119 2.711
M**2/HZ
WAVE SPECTRAL DENSITY
50.
40.
30.
20.
10.
0.
0.
0.1
0.2
0.3
0.4
0.5
0.6
0.7
FREQUENCY HZ

Fig.

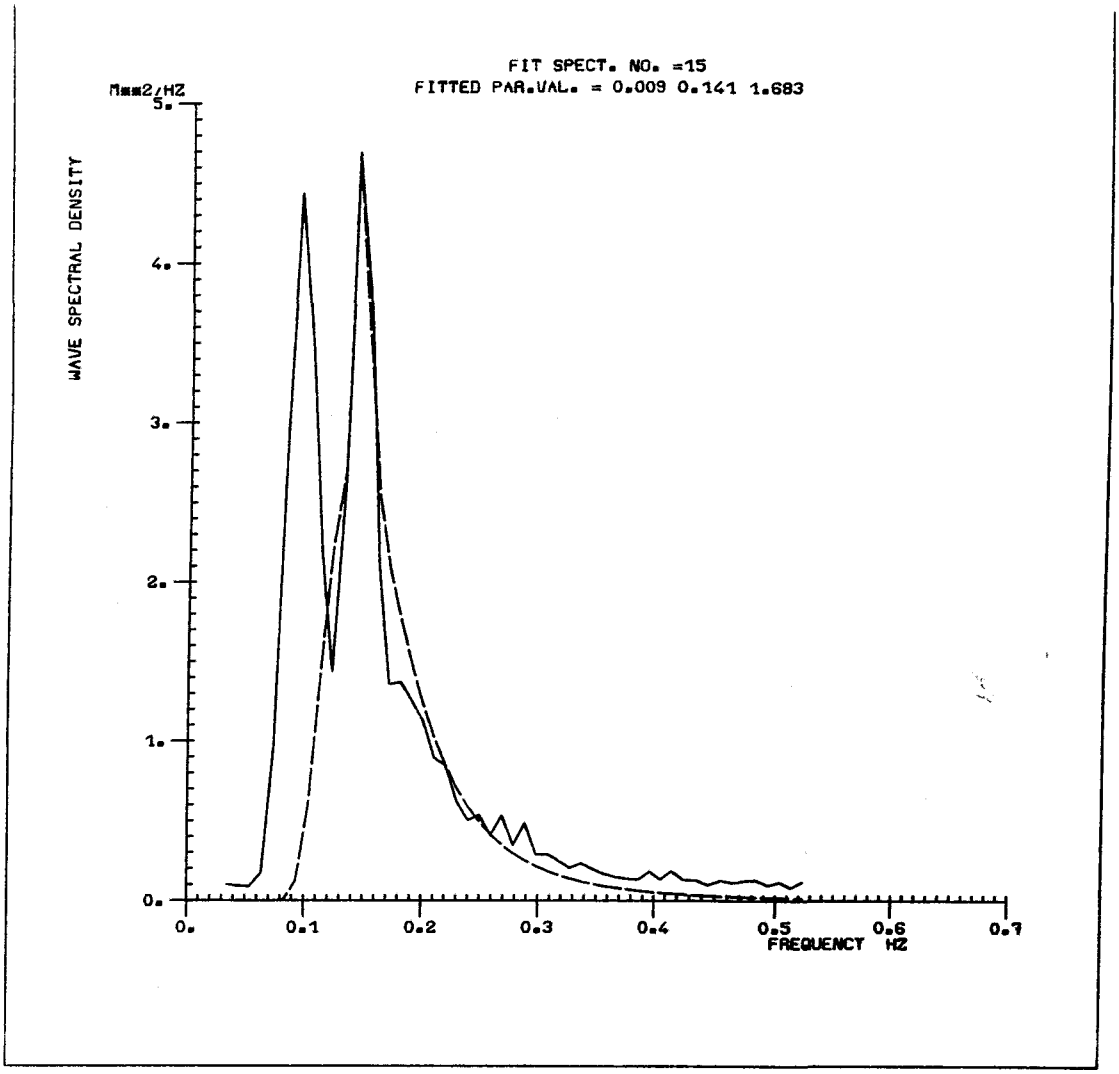
FIT SPECT. NO. =15
FITTED PAR.VAL. = 0.009 0.141 1.683
MM**2/HZ
WAVE SPECTRAL DENSITY
5.
4.
3.
2.
1.
0.
0.
0.1
0.2
0.3
0.4
0.5
0.6
0.7
FREQUENCY HZ

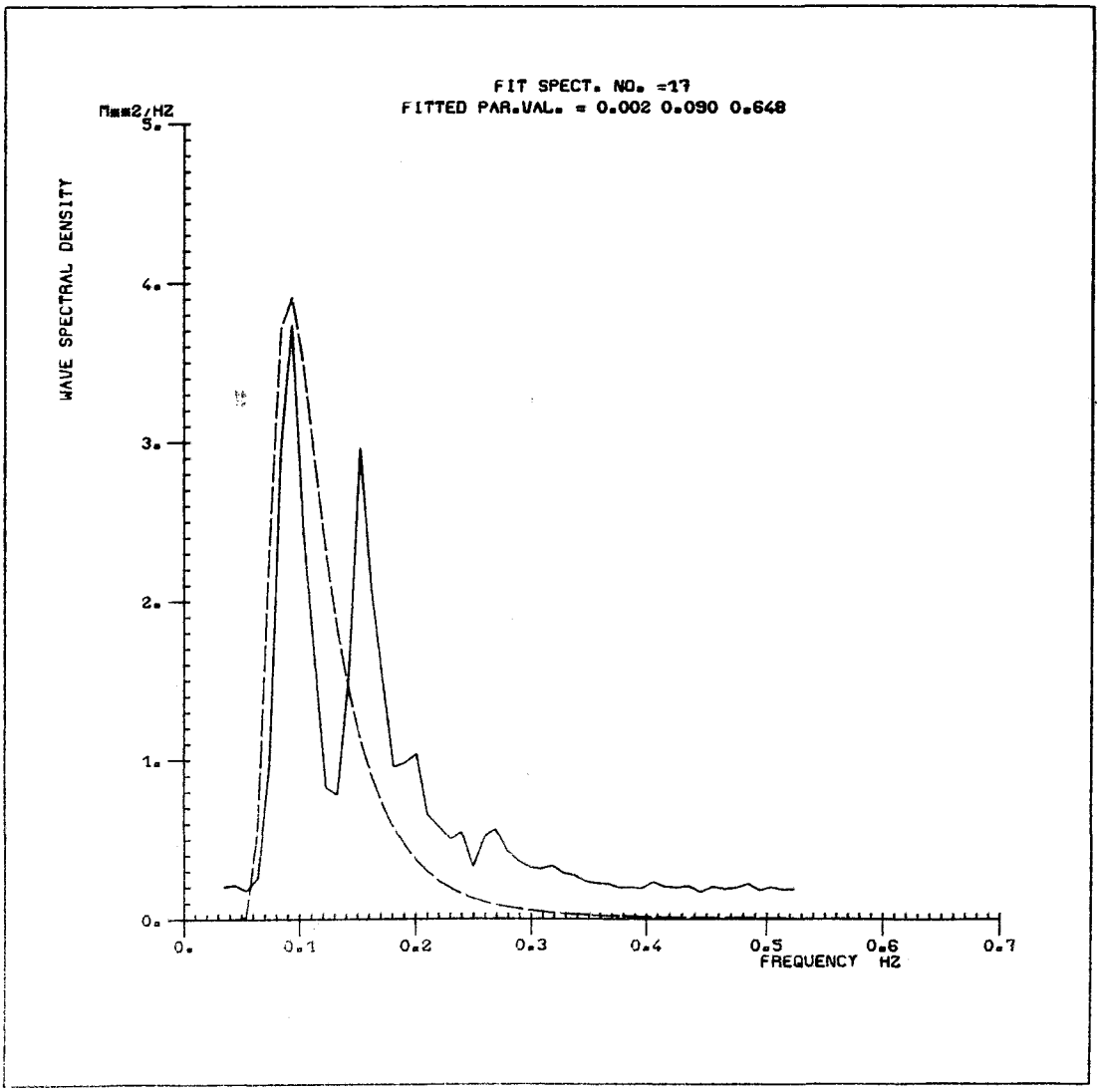
FIT SPECT. NO. =17
FITTED PAR.VAL. = 0.002 0.090 0.648
MM**2/HZ
WAVE SPECTRAL DENSITY
5.
4.
3.
2.
1.
0.
0.
0.1
0.2
0.3
0.4
0.5
0.6
0.7
FREQUENCY HZ

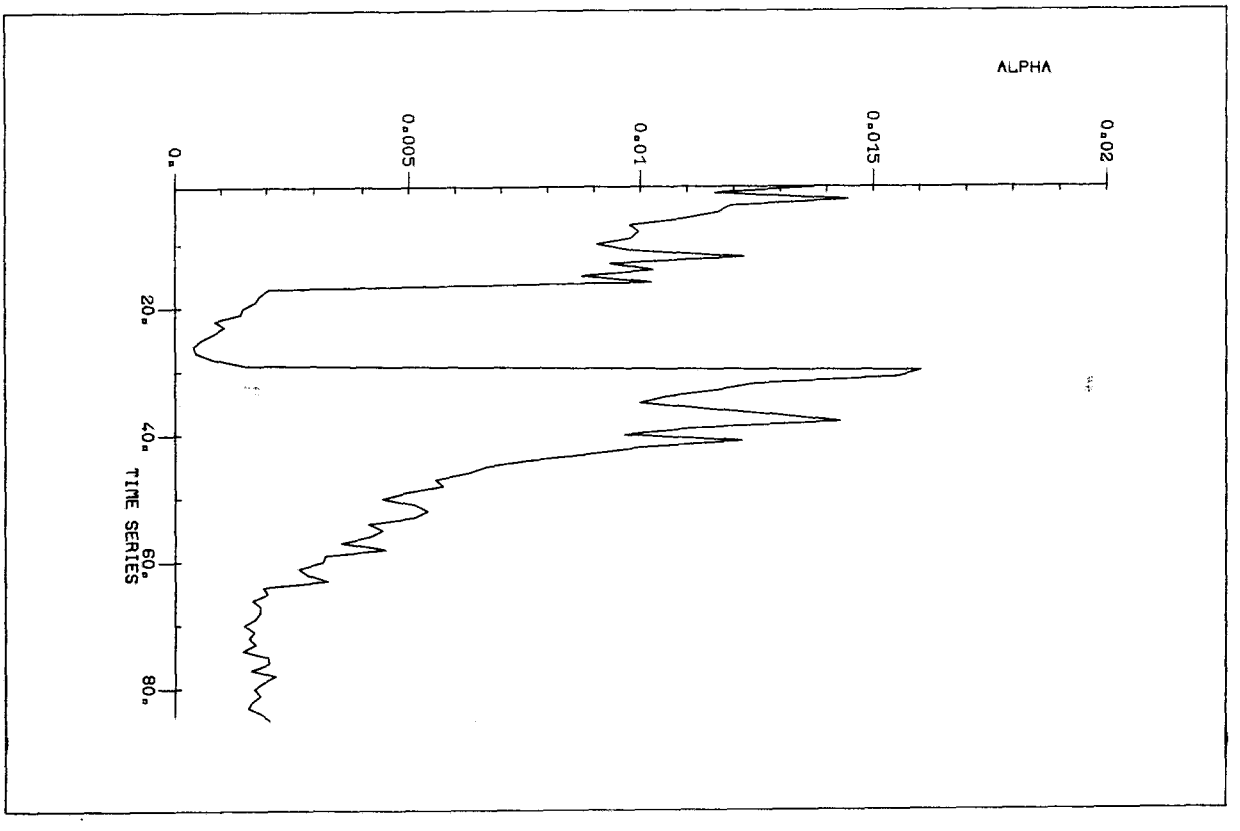
ALPHA
0.
0.005
0.01
0.015
0.02
20.
40.
60.
80.
TIME SERIES

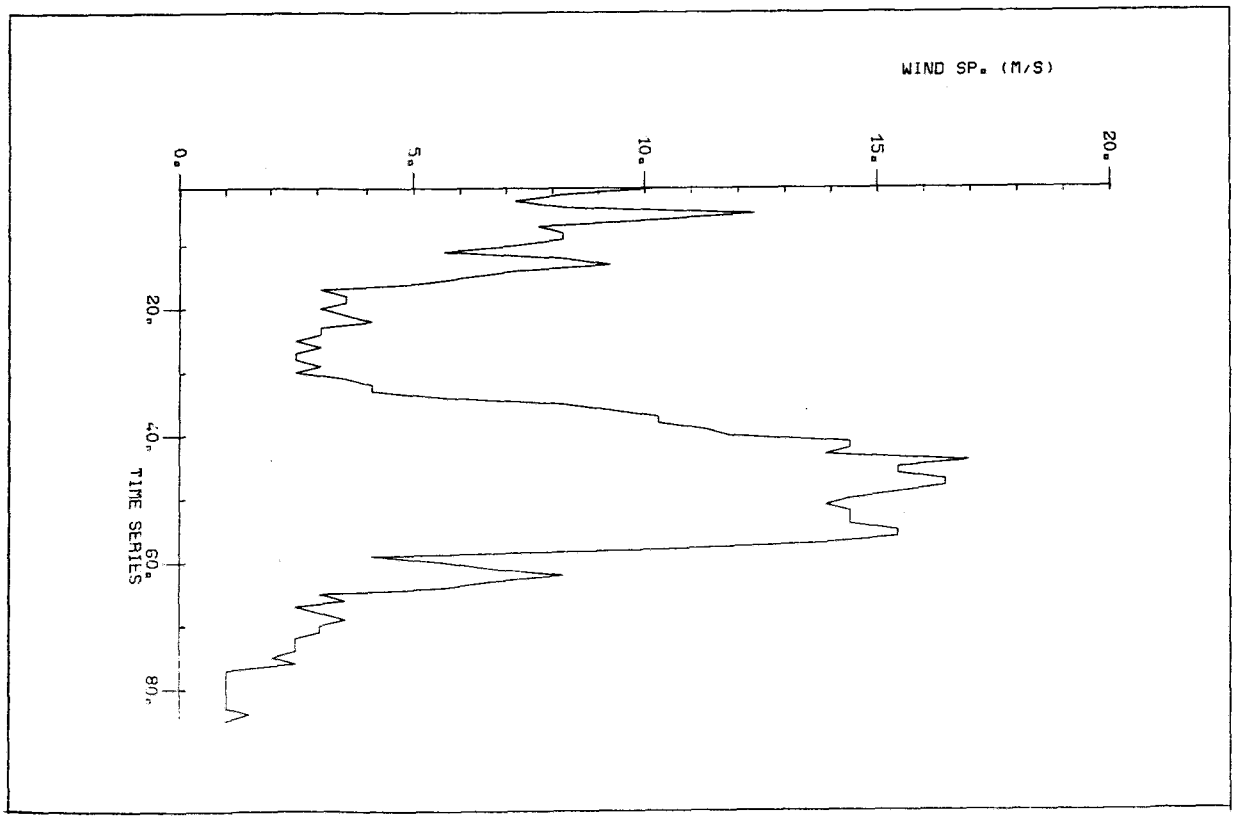
WIND SP. (M/S)
0.
5.
10.
15.
20.
20.
40.
60.
80.
TIME SERIES

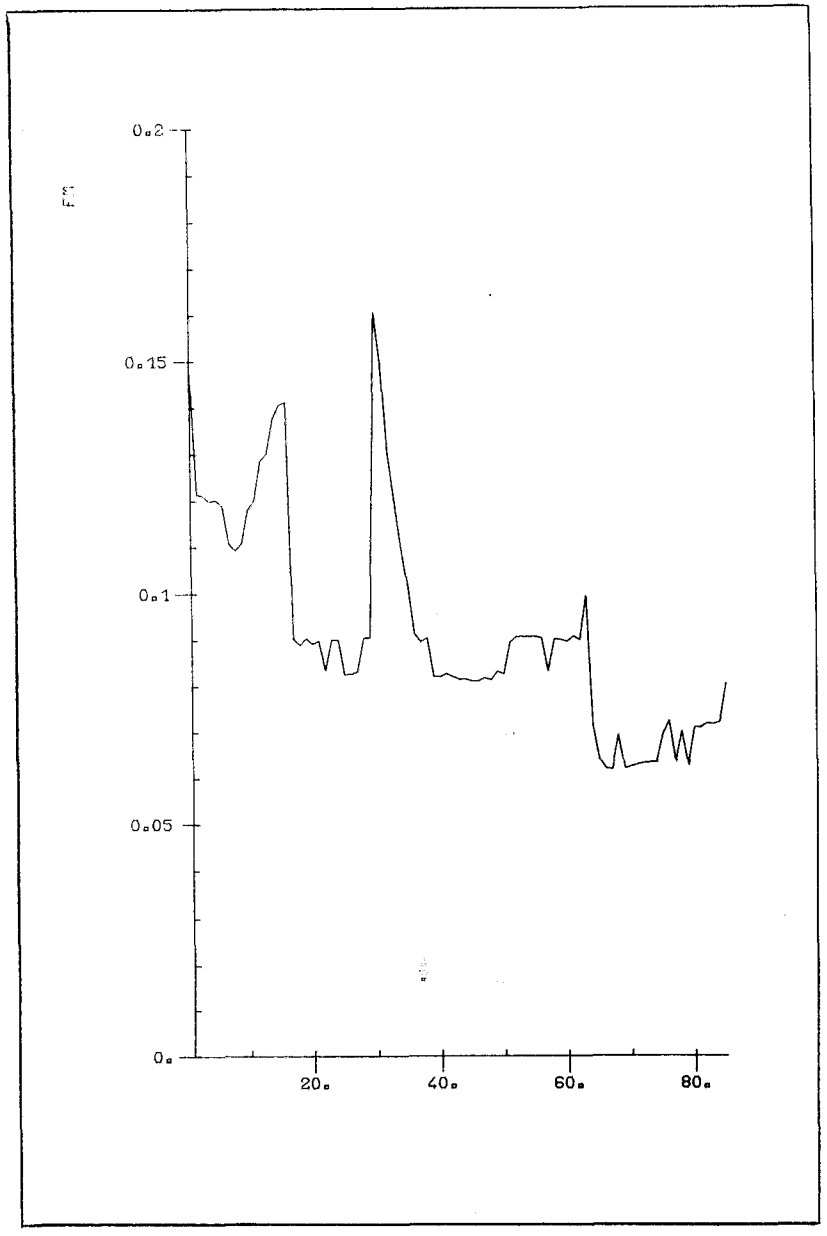
FM
0.2
0.15
0.1
0.05
0.
20.
40.
60.
80.

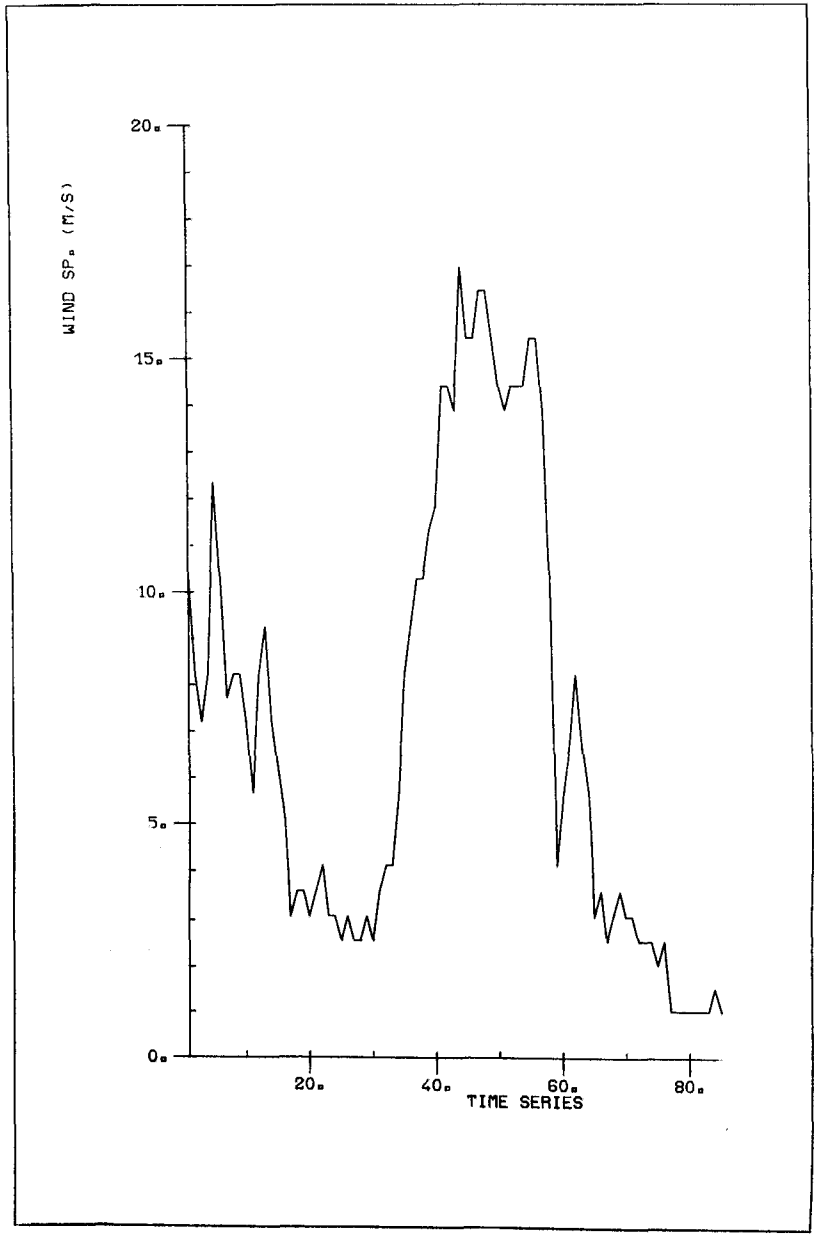
WIND SP. (M/S)
20.
15.
10.
5.
0.
20.
40.
60.
80.
TIME SERIES

Fig. 19

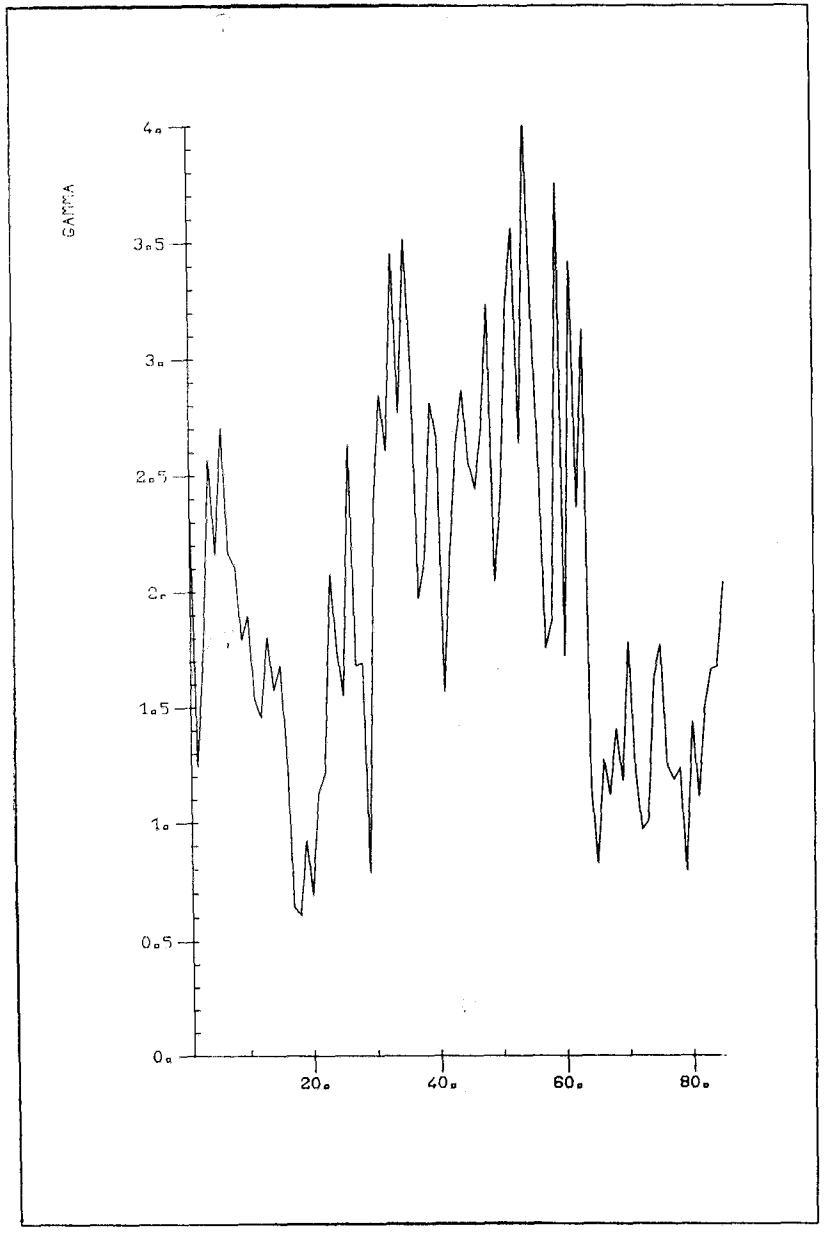
GAMMA
4.
3.5
3.
2.5
2.
1.5
1.
0.5
0.
20.
40.
60.
80.

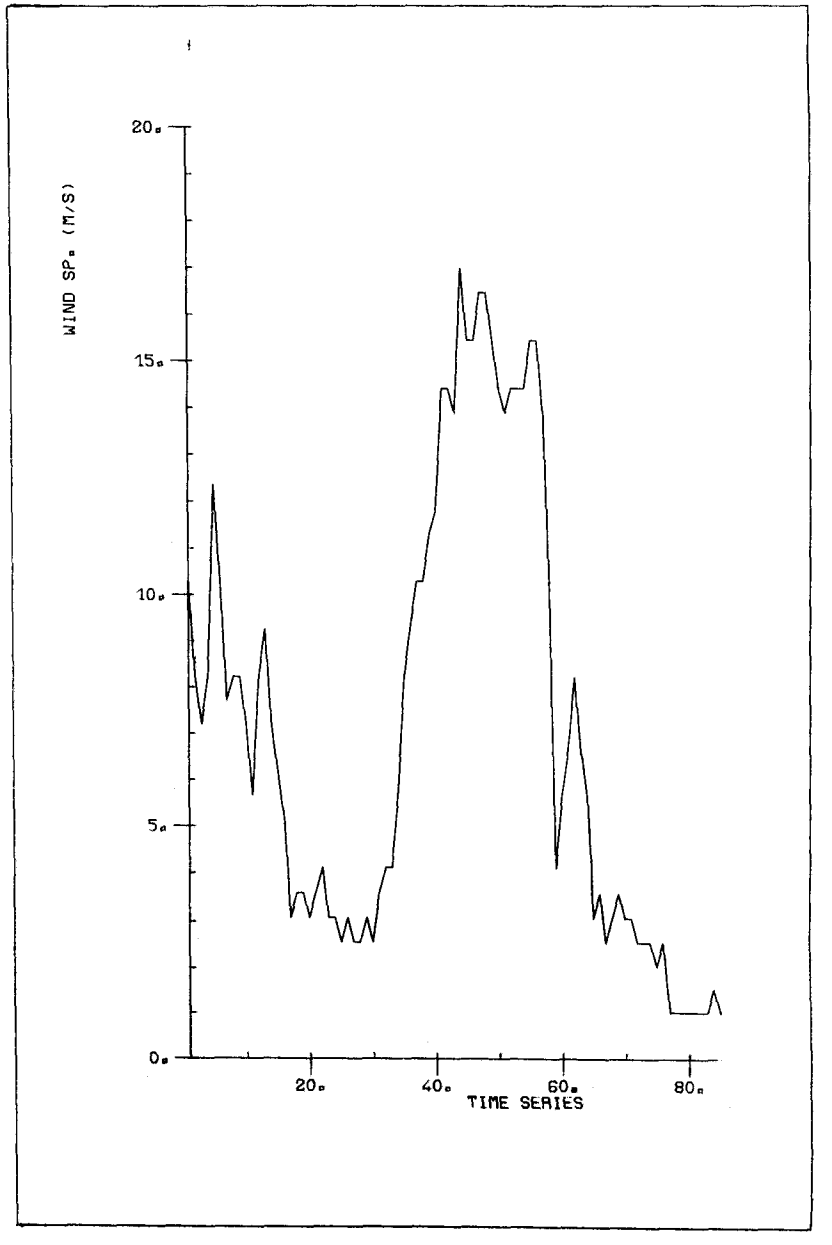
WIND SP. (M/S)
20.
15.
10.
5.
0.
20.
40.
60.
80.
TIME SERIES

Fig. 2c

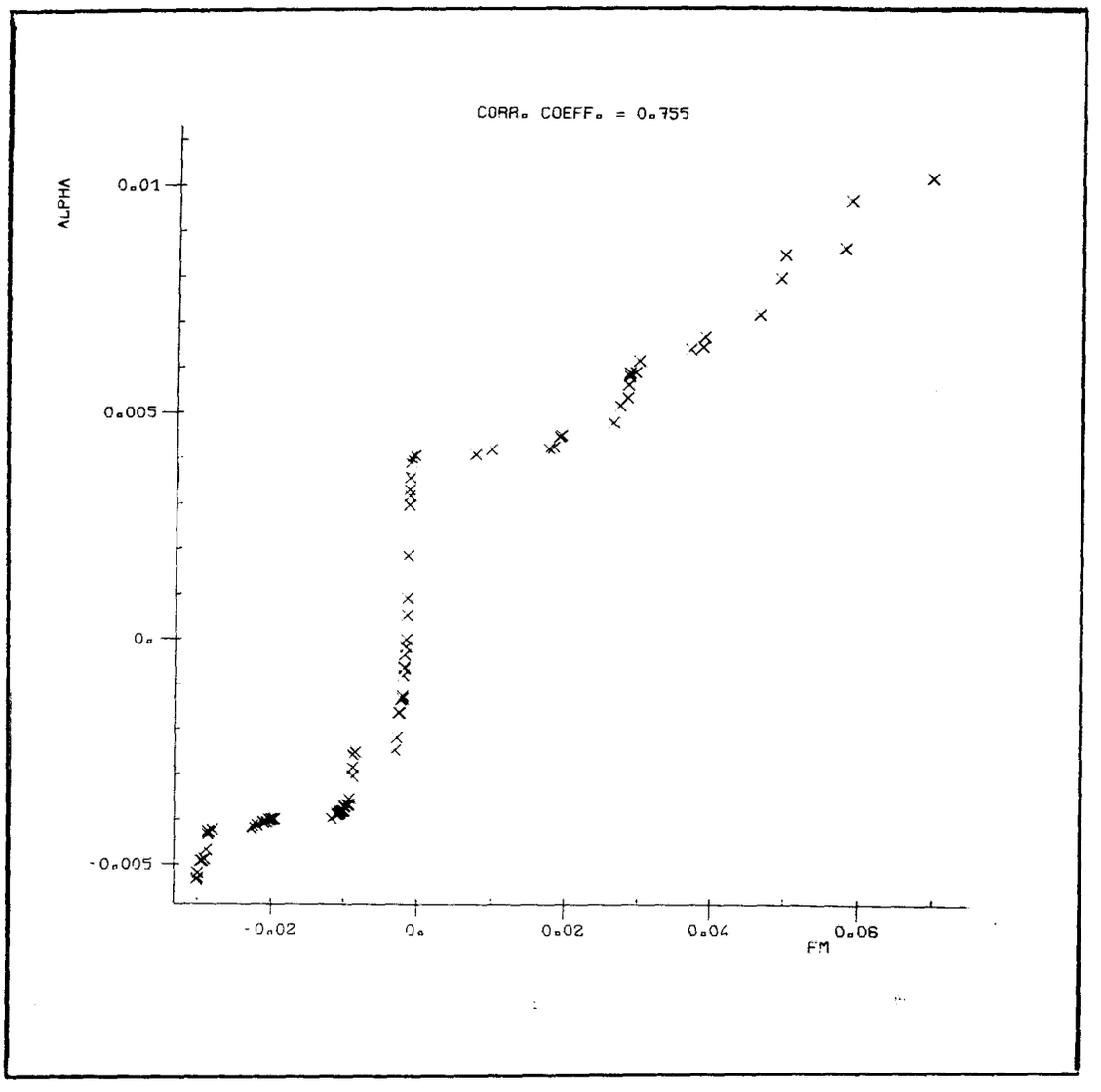

Fig. 21

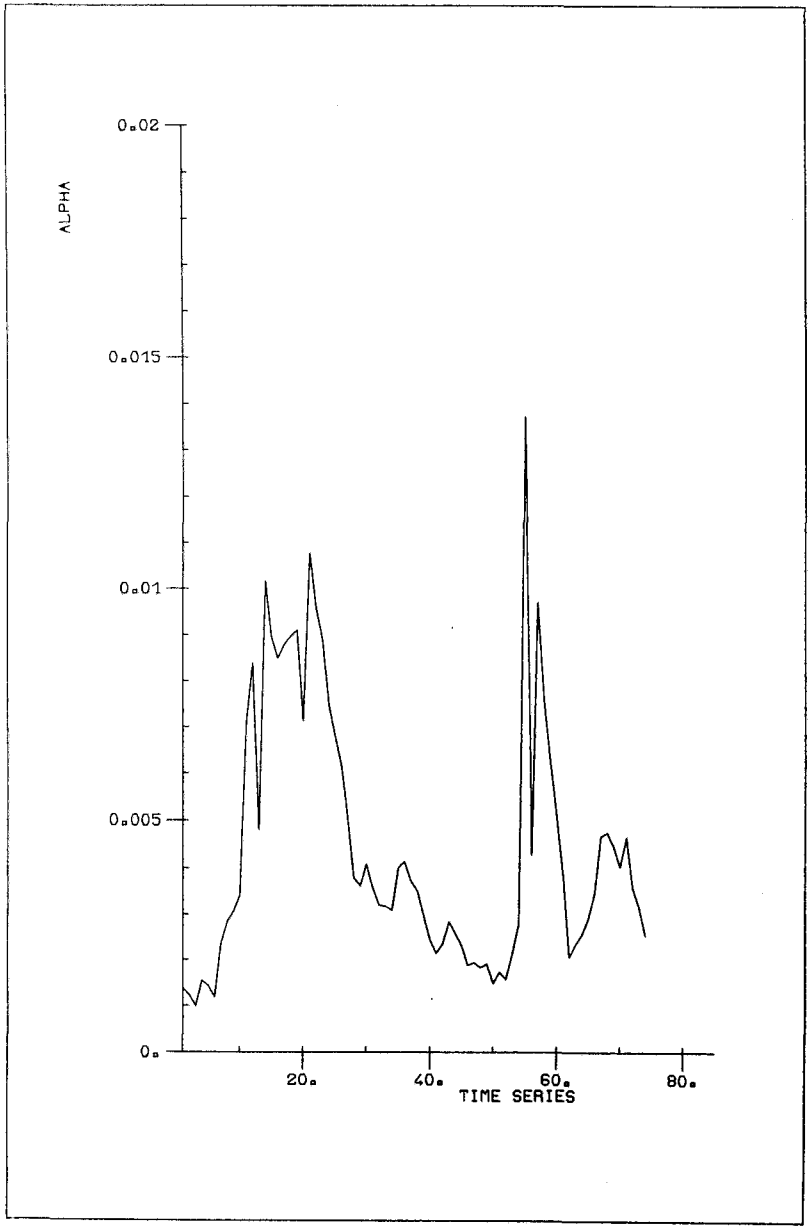
ALPHA
0.02
0.015
0.01
0.005
0.
20.
40.
60.
80.
TIME SERIES

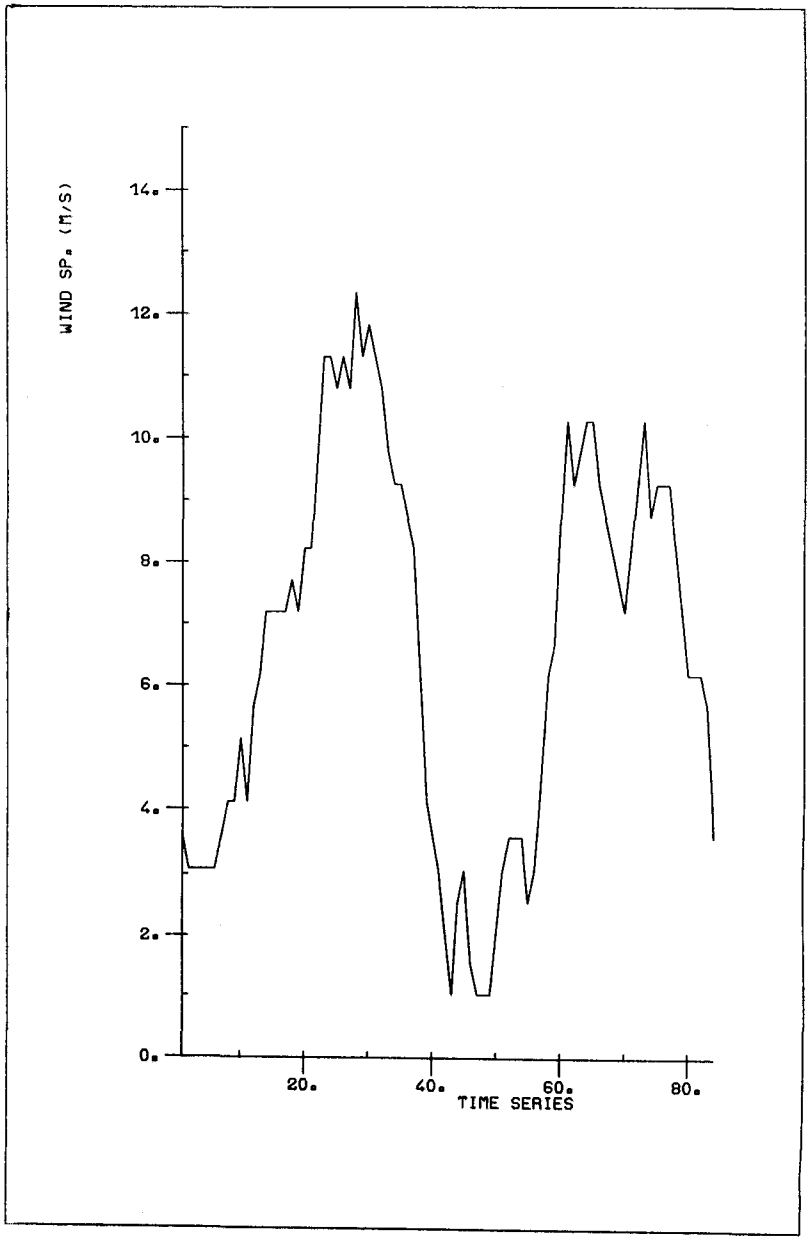
WIND SP. (M/S)
14.
12.
10.
8.
6.
4.
2.
0.
20.
40.
60.
80.
TIME SERIES

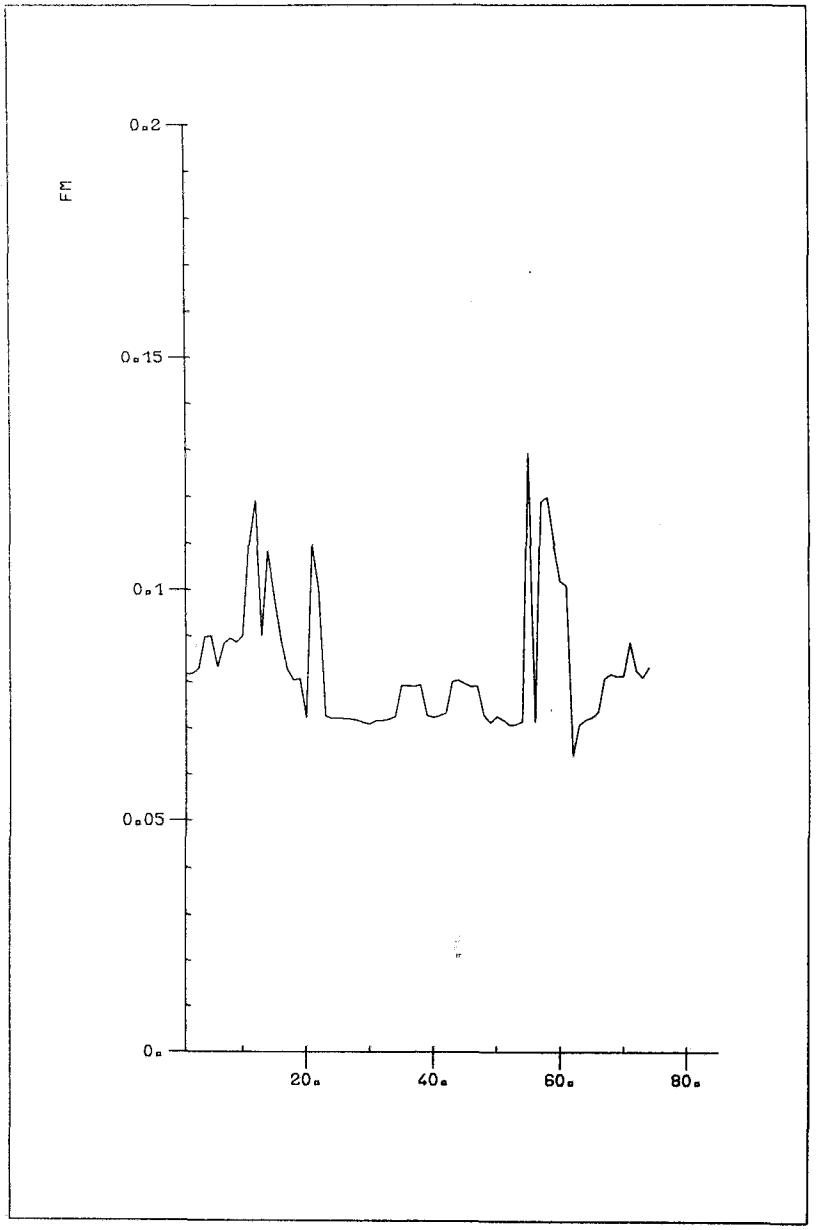
FM
0.2
0.15
0.1
0.05
0.
20.
40.
60.
80.

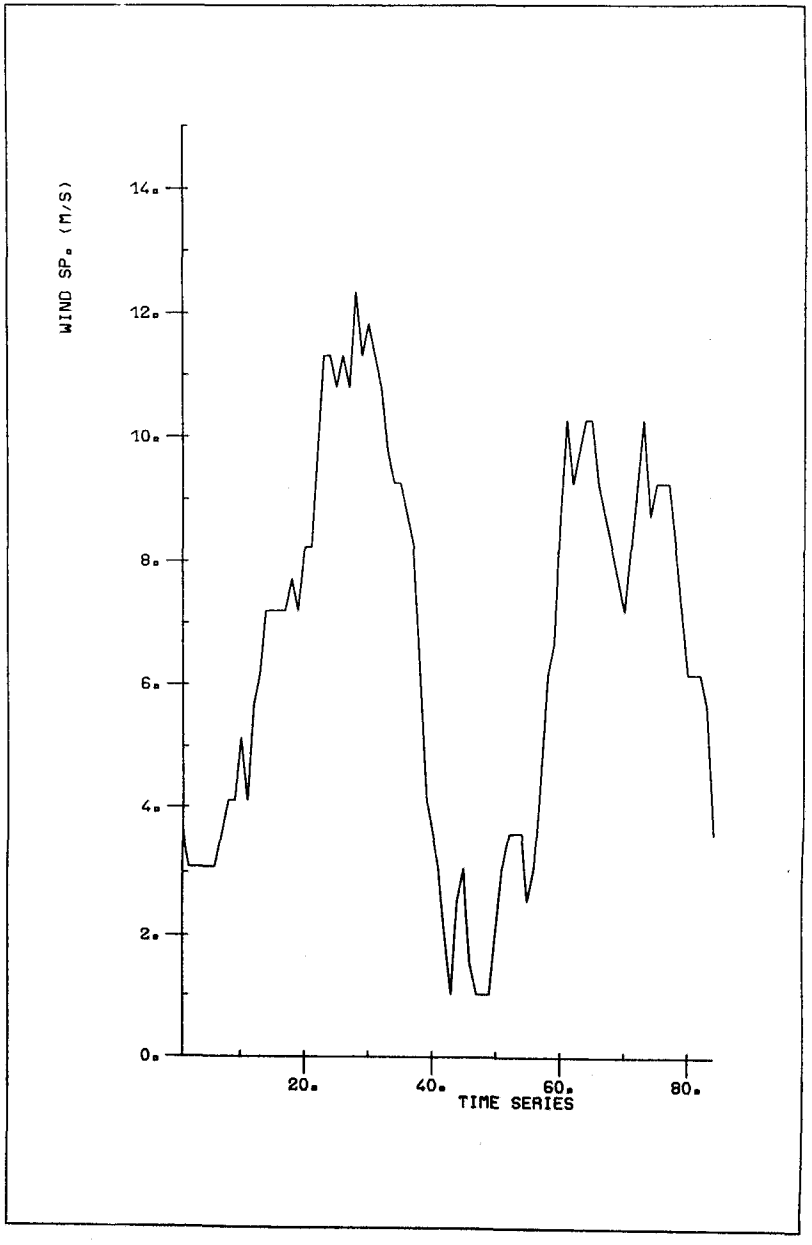
WIND SP. (M/S)
14.
12.
10.
8.
6.
4.
2.
0.
20.
40.
60.
80.
TIME SERIES

Fig. 23

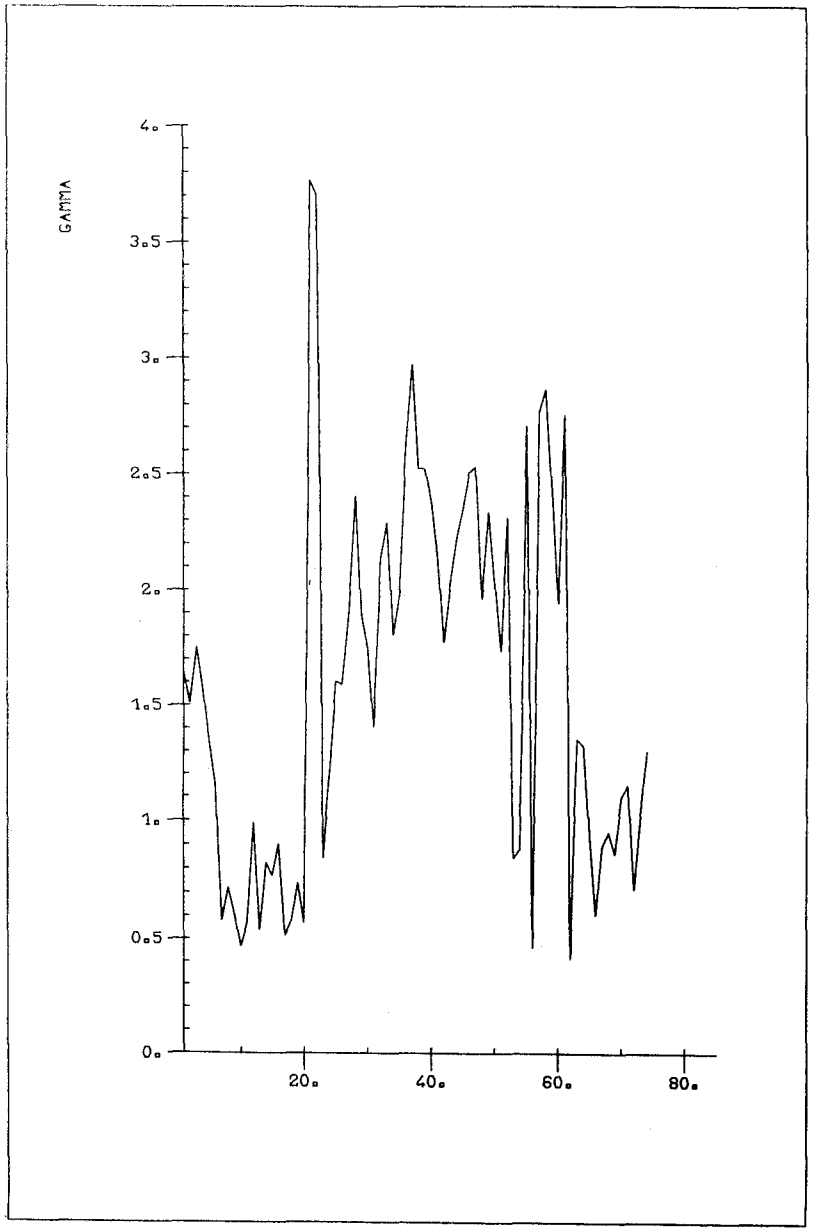
GAMMA
4.
3.5
3.
2.5
2.
1.5
1.
0.5
0.
20.
40.
60.
80.

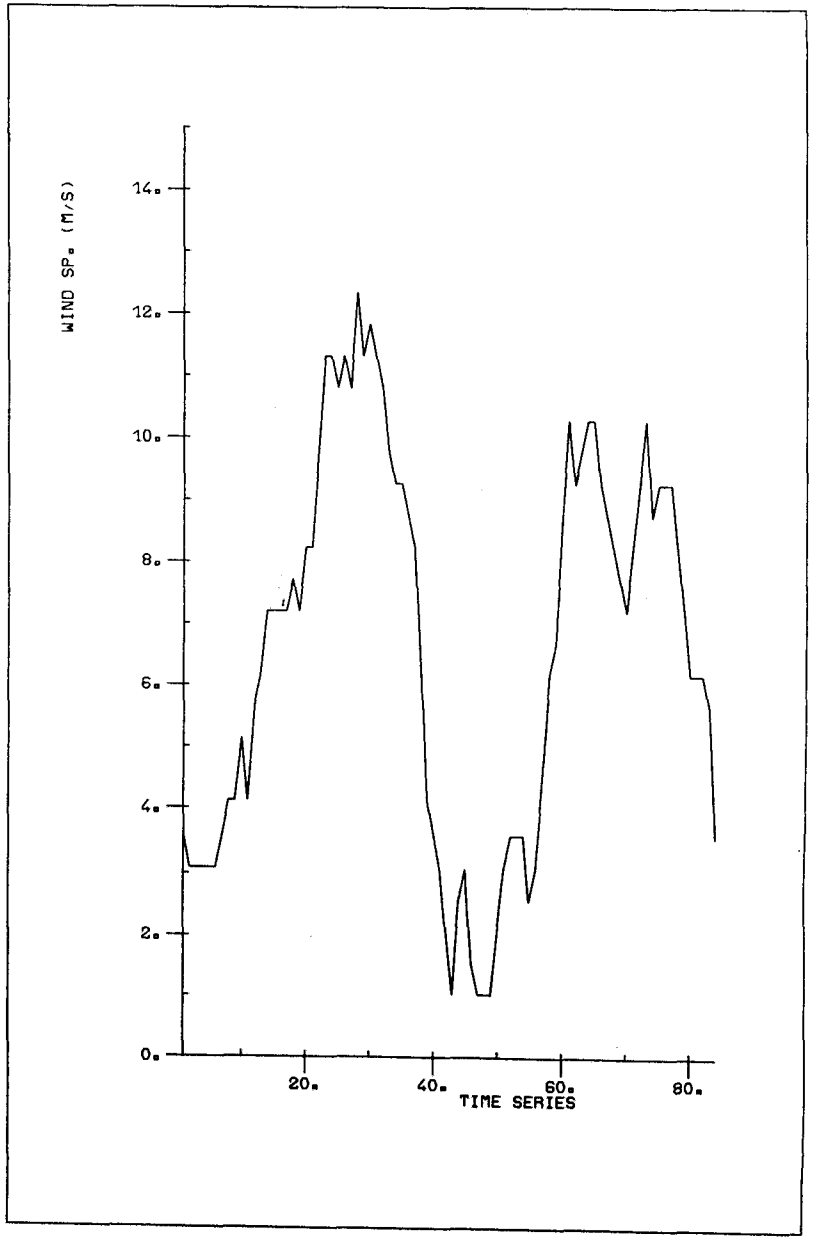
WIND SP. (M/S)
14.
12.
10.
8.
6.
4.
2.
0.
20.
40.
60.
80.
TIME SERIES

Fig. 2

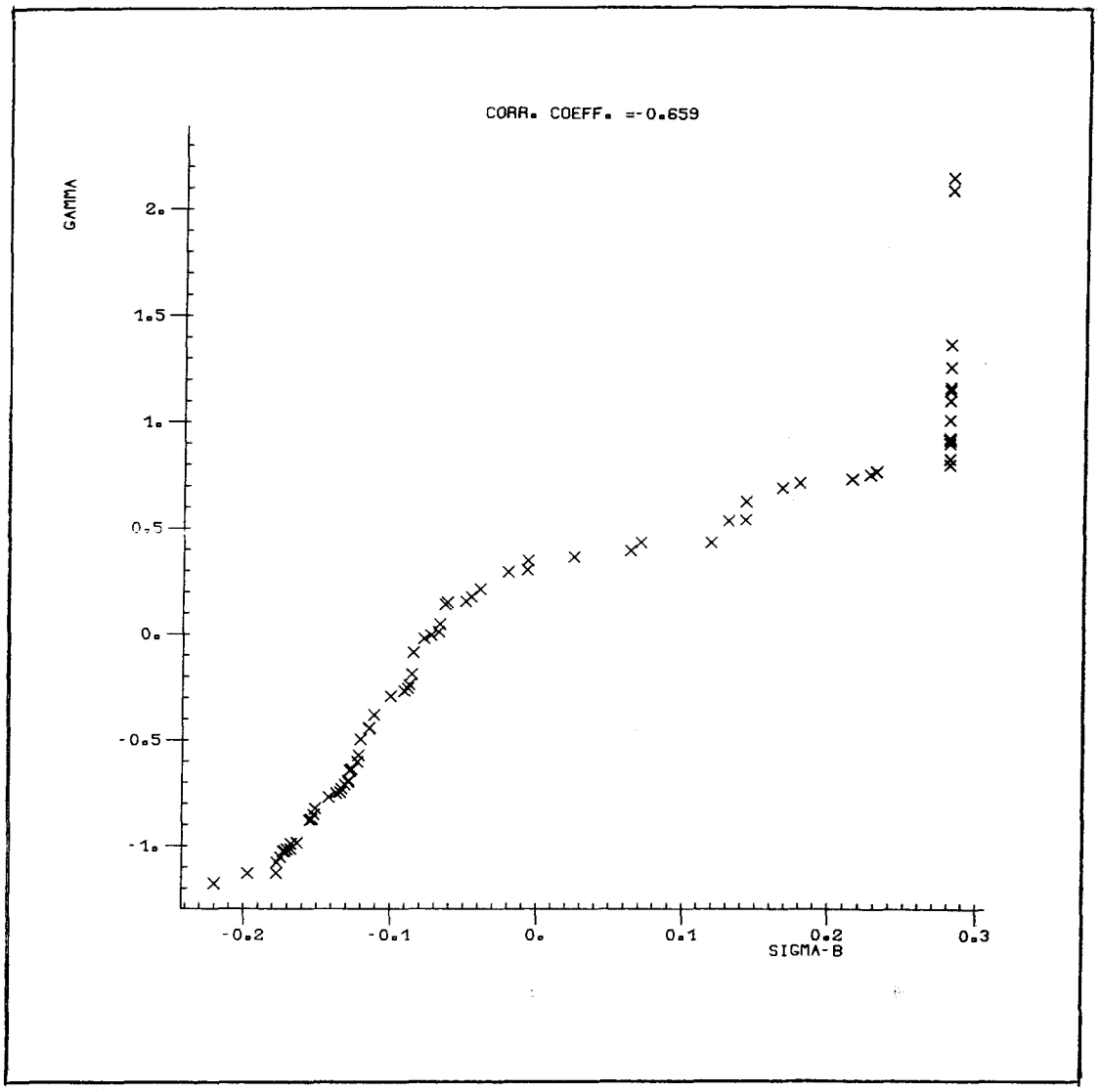

Fig. 25

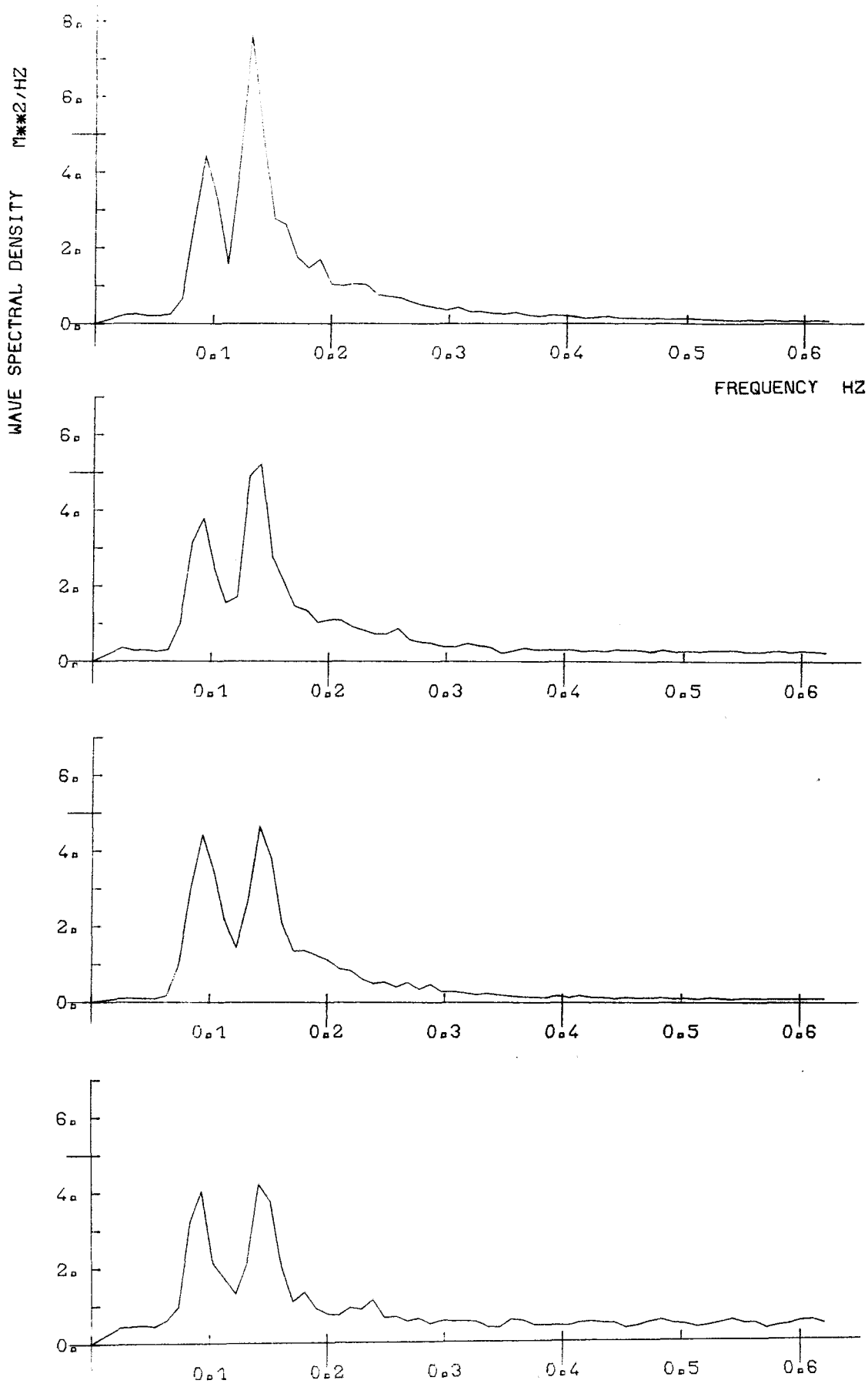
WAVE SPECTRAL DENSITY M**2/HZ
8.
6.
4.
2.
0.
0.1
0.2
0.3
0.4
0.5
0.6
FREQUENCY HZ

Fig. 4

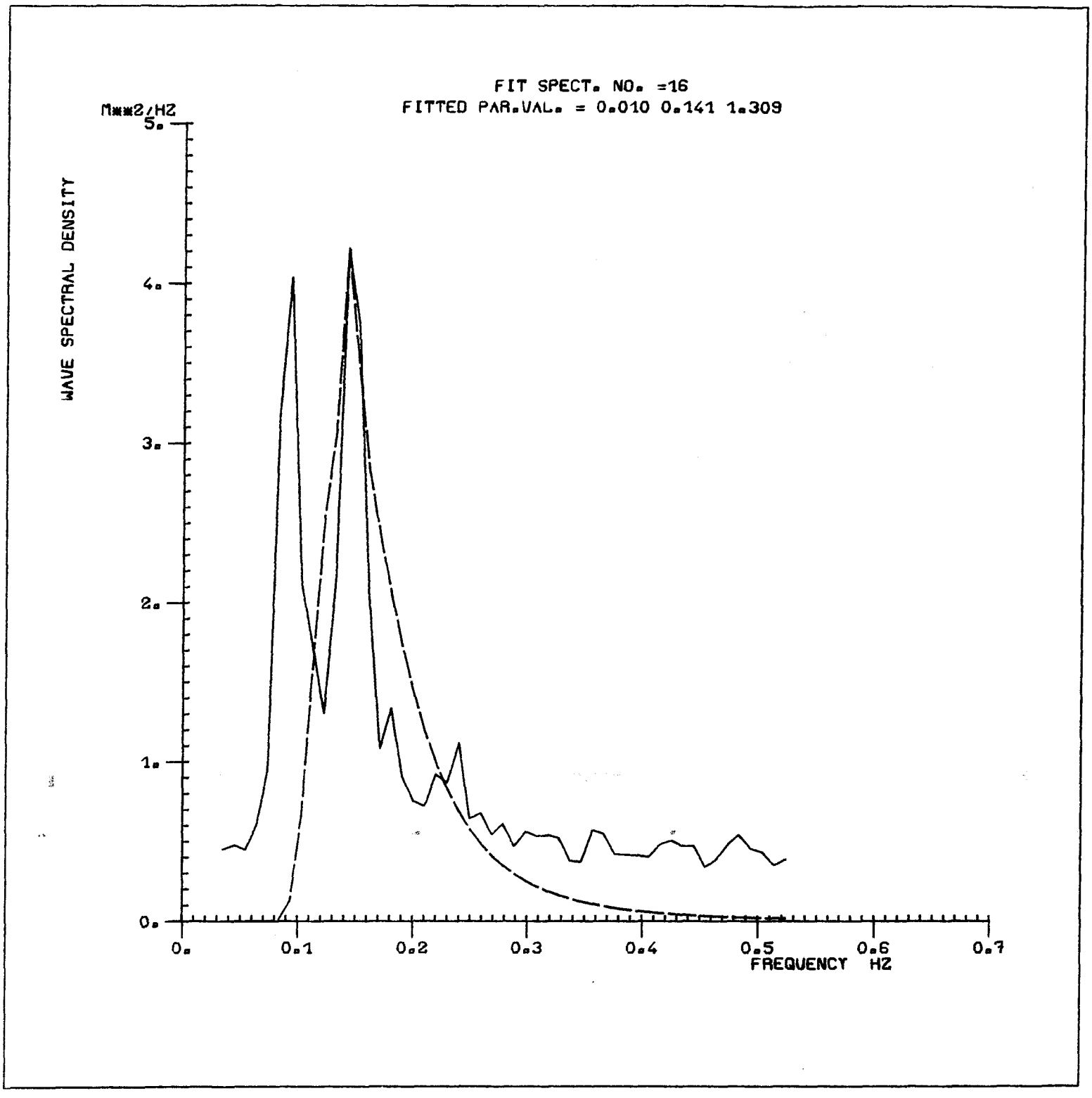
FIT SPECT. NO. =16
FITTED PAR.VAL. = 0.010 0.141 1.309
M**2/HZ
WAVE SPECTRAL DENSITY
5.
4.
3.
2.
1.
0.
0.
0.1
0.2
0.3
0.4
0.5
0.6
0.7
FREQUENCY HZ

Fig. 2

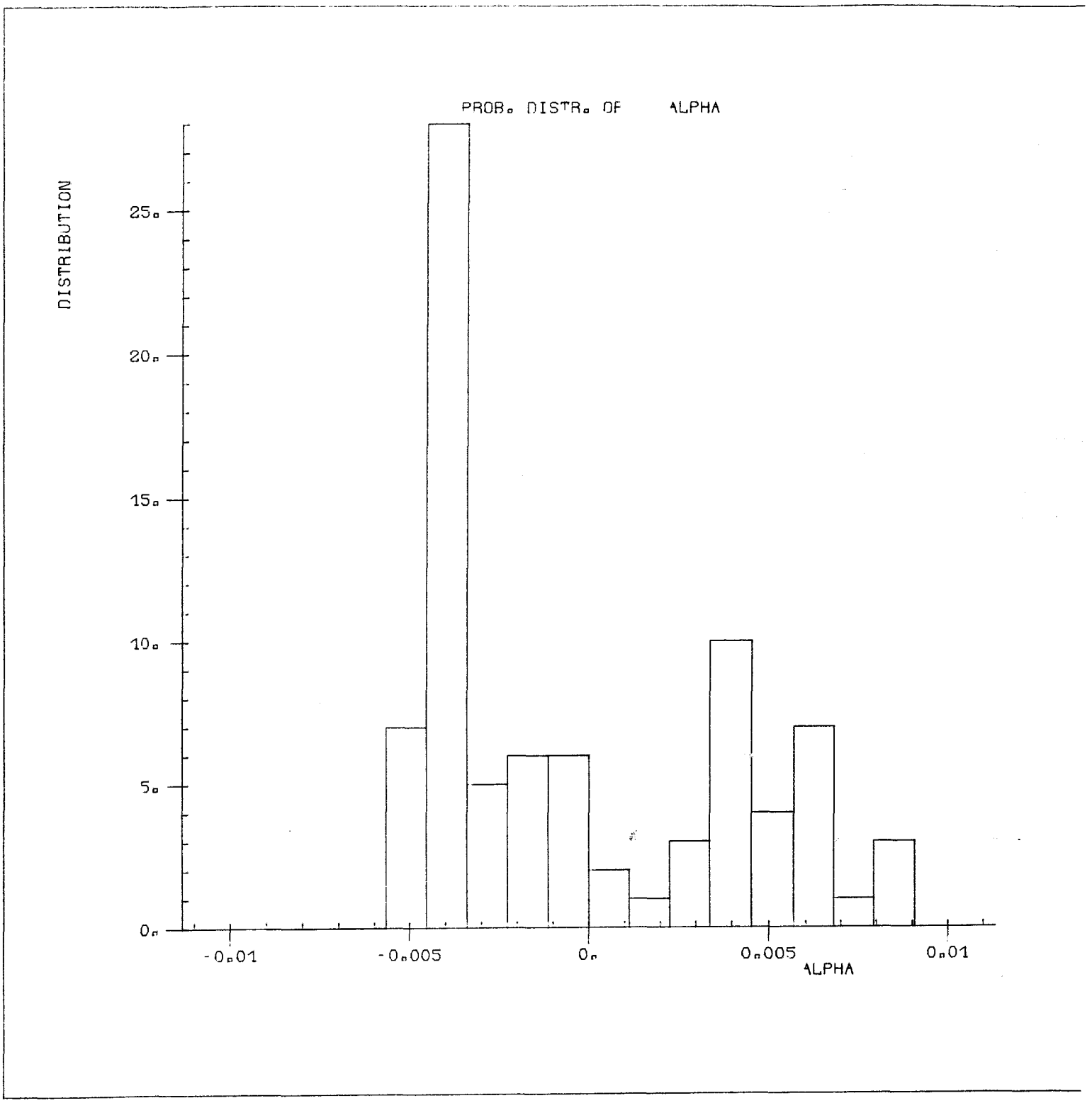
PROB. DISTR. OF ALPHA
DISTRIBUTION
25.
20.
15.
10.
5.
0.
-0.01
-0.005
0.
0.005
0.01
ALPHA

Fig. 2

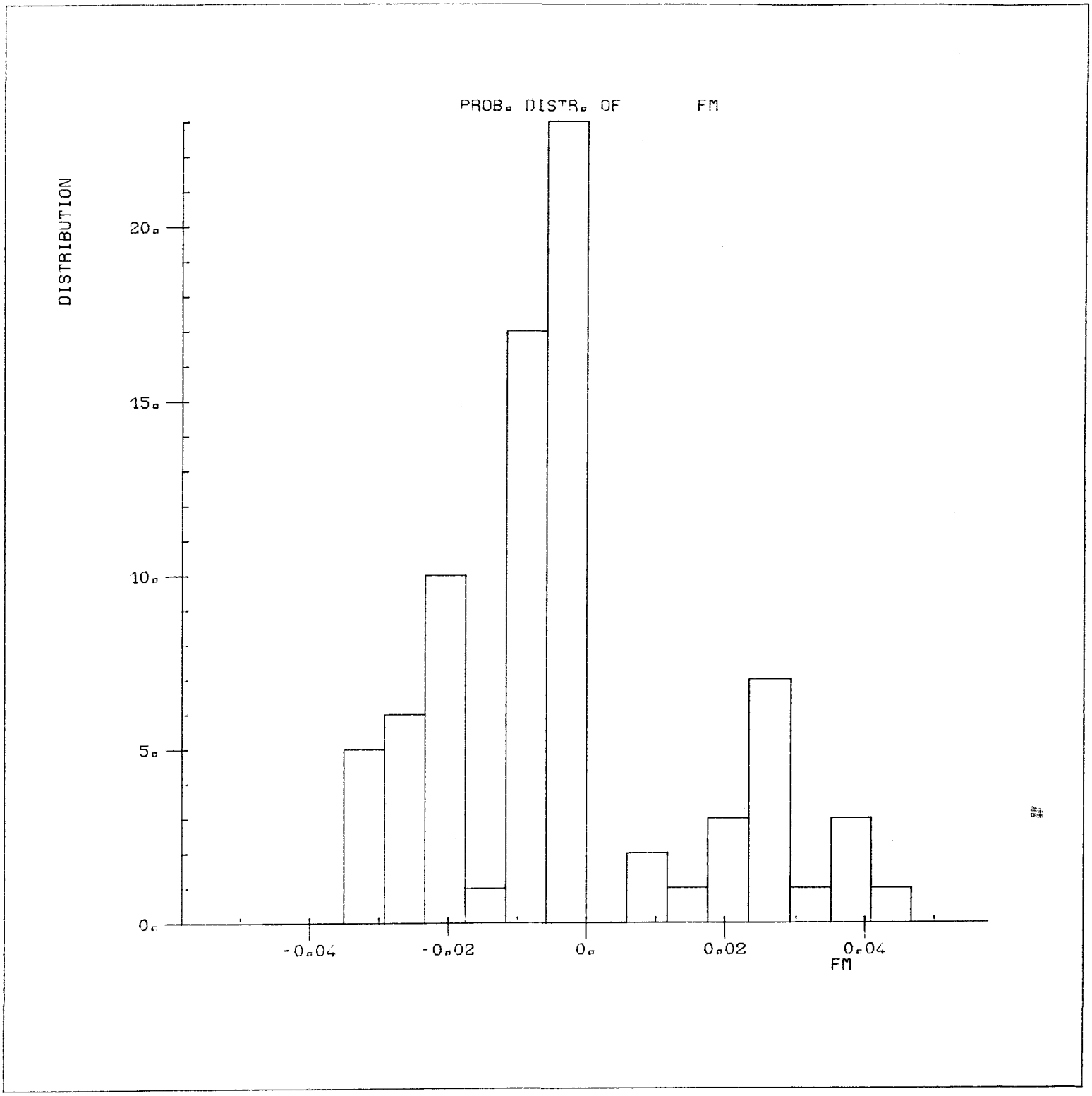

Fig. 2

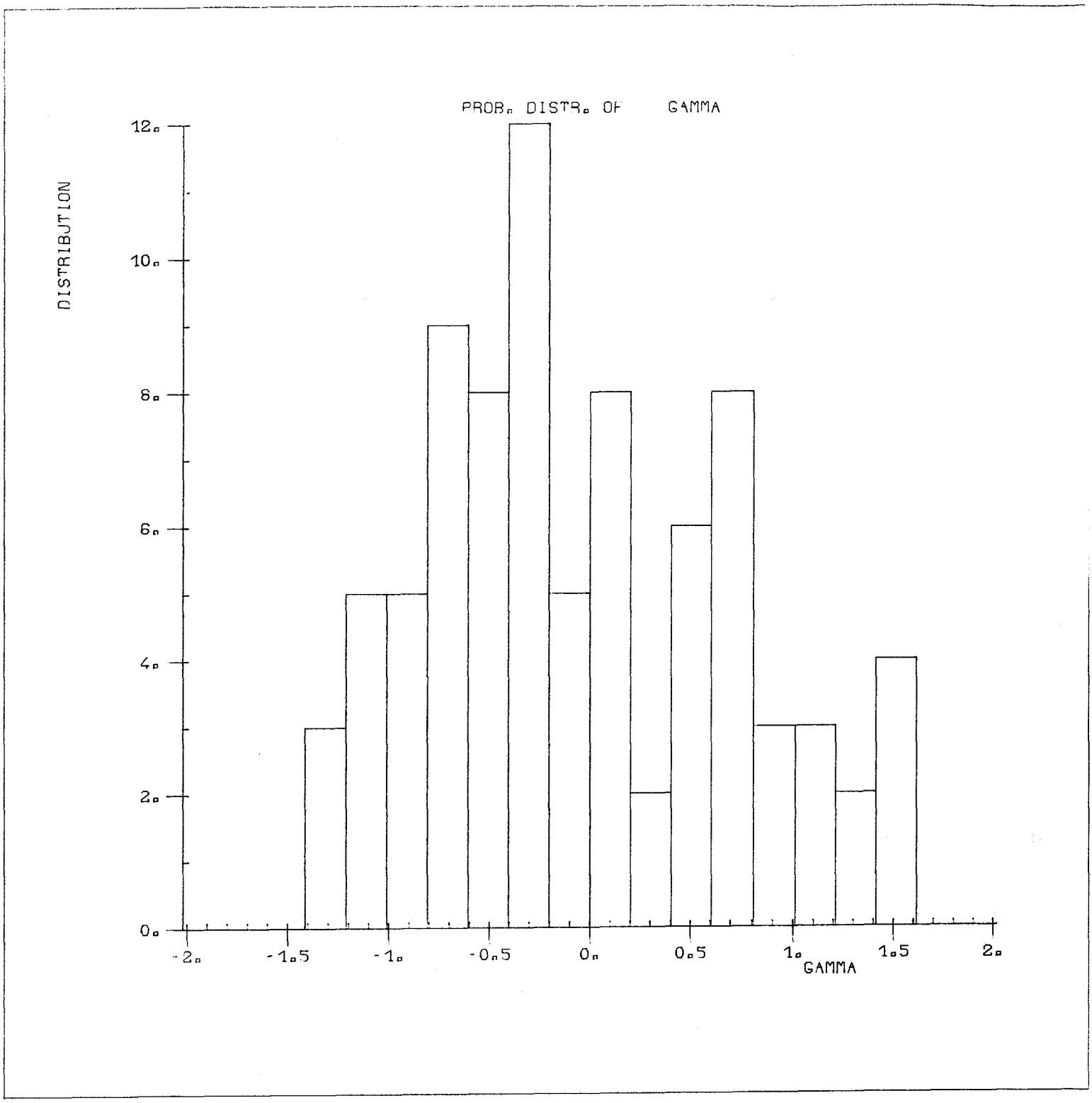
PROB. DISTR. OF GAMMA
DISTRIBUTION
12.
10.
8.
6.
4.
2.
0.
-2.
-1.5
-1.
-0.5
0.
0.5
1.
1.5
2.
GAMMA

Fig. 3

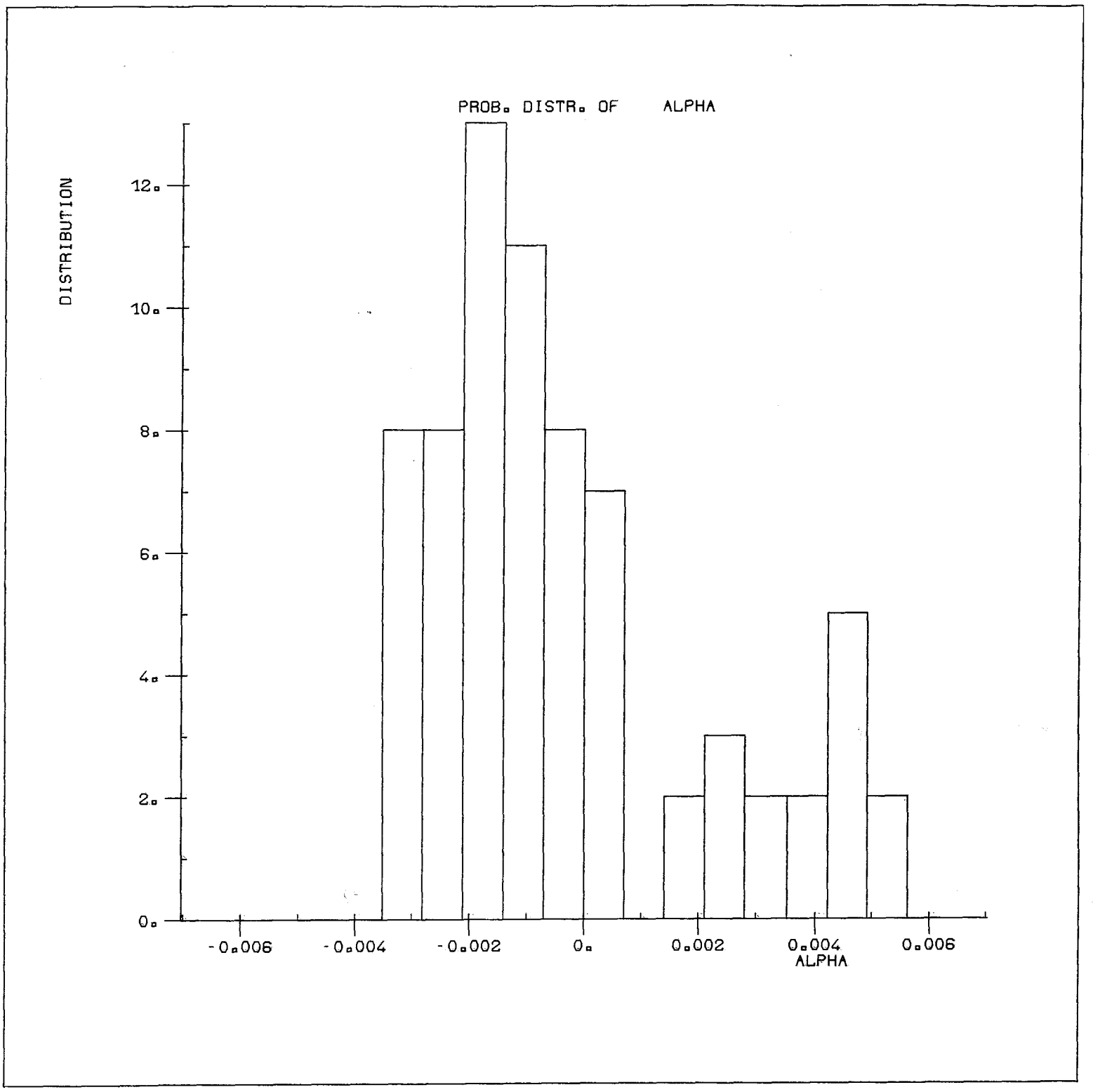
PROB. DISTR. OF ALPHA
DISTRIBUTION
12.
10.
8.
6.
4.
2.
0.
-0.006
-0.004
-0.002
0.
0.002
0.004
0.006
ALPHA

Fig-31

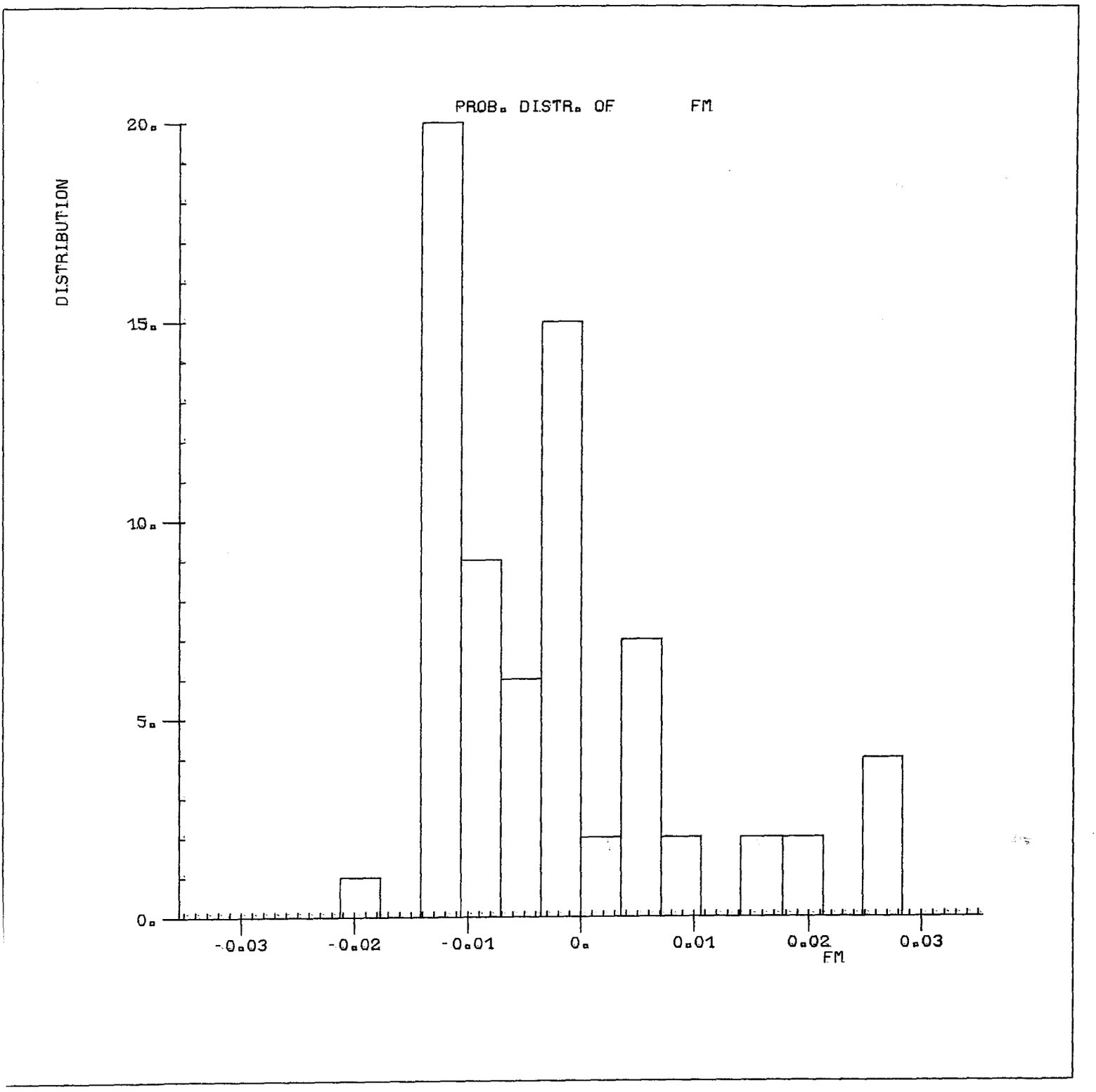
PROB. DISTR. OF FM
DISTRIBUTION
20.
15.
10.
5.
0.
-0.03
-0.02
-0.01
0.
0.01
0.02
0.03
FM

Fig. 3

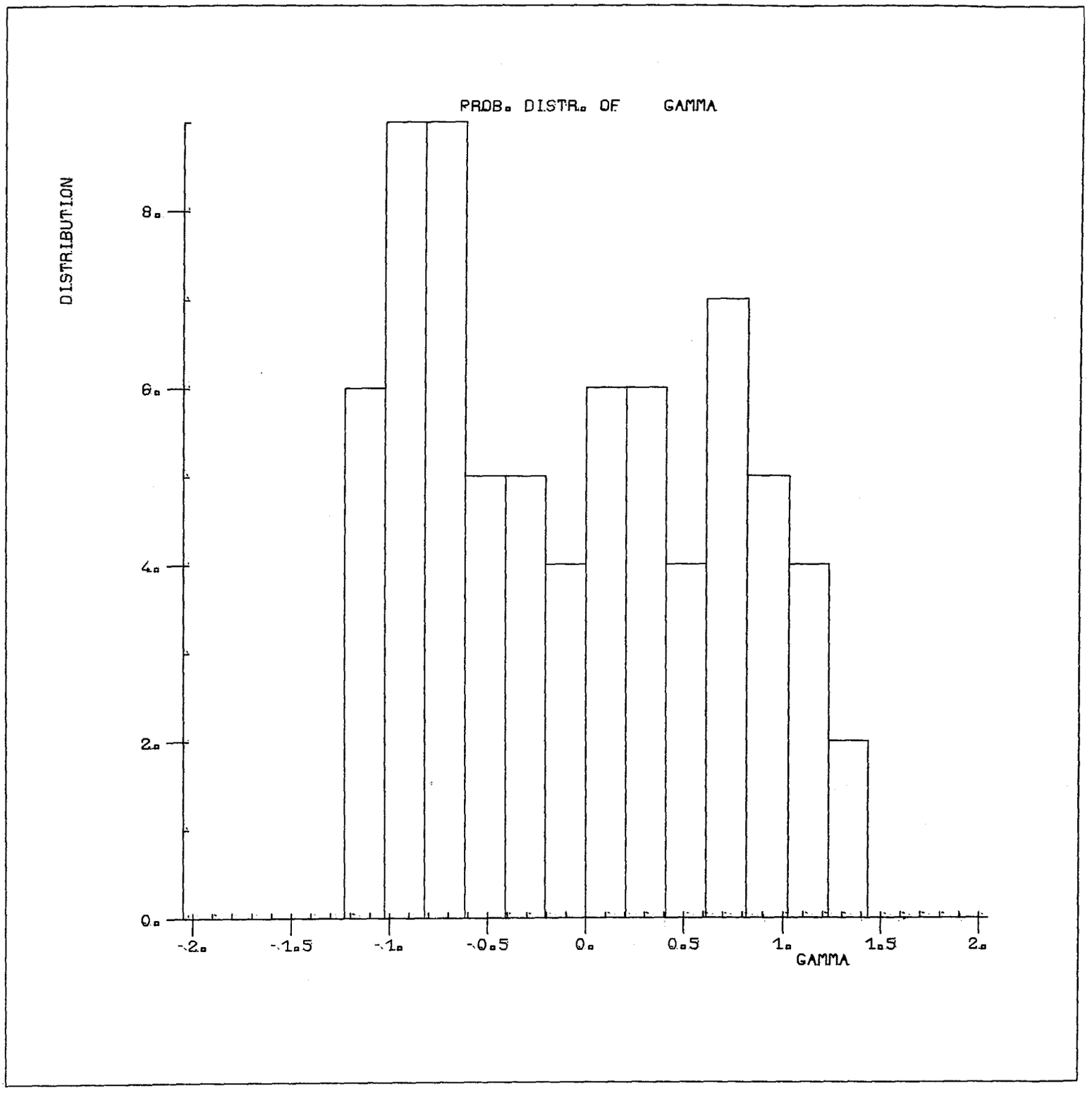
PROB. DISTR. OF GAMMA
DISTRIBUTION
8.
6.
4.
2.
0.
-2.
-1.5
-1.
-0.5
0.
0.5
1.
1.5
2.
GAMMA